Am J Physiol Gastrointest Liver Physiol 314: G517–G536, 2018.
First published November 22, 2017; doi:10.1152/ajpgi.00135.2017.

RESEARCH ARTICLE | *Pancreatic Physiology/Pathophysiology*

Exocrine pancreas glutamate secretion help to sustain enterocyte nutritional needs under protein restriction

S. Araya,[1] E. Kuster,[1] D. Gluch,[1] L. Mariotta,[1] C. Lutz,[1] T. V. Reding,[2] R. Graf,[2] F. Verrey,[1] and S. M. R. Camargo[1]

[1]*Institute of Physiology and Zurich Center for Integrative Human Physiology, University of Zurich, Zurich, Switzerland; and* [2]*Department of Surgery, University Hospital Zurich, Zurich, Switzerland*

Submitted 25 April 2017; accepted in final form 17 November 2017

Araya S, Kuster E, Gluch D, Mariotta L, Lutz C, Reding TV, Graf R, Verrey F, Camargo SM. Exocrine pancreas glutamate secretion help to sustain enterocyte nutritional needs under protein restriction. *Am J Physiol Gastrointest Liver Physiol* 314: G517–G536, 2018. First published November 22, 2017; doi:10.1152/ajpgi.00135.2017.—Glutamine (Gln) is the most concentrated amino acid in blood and considered conditionally essential. Its requirement is increased during physiological stress, such as malnutrition or illness, despite its production by muscle and other organs. In the malnourished state, Gln has been suggested to have a trophic effect on the exocrine pancreas and small intestine. However, the Gln transport capacity, the functional relationship of these two organs, and the potential role of the Gln-glutamate (Glu) cycle are unknown. We observed that pancreatic acinar cells express lower levels of Glu than Gln transporters. Consistent with this expression pattern, the rate of Glu influx into acinar cells was approximately sixfold lower than that of Gln. During protein restriction, acinar cell glutaminase expression was increased and Gln accumulation was maintained. Moreover, Glu secretion by acinar cells into pancreatic juice and thus into the lumen of the small intestine was maintained. In the intestinal lumen, Glu absorption was preserved and Glu dehydrogenase expression was augmented, potentially providing the substrates for increasing energy production via the TCA cycle. Our findings suggest that one mechanism by which Gln exerts a positive effect on exocrine pancreas and small intestine involves the Gln metabolism in acinar cells and the secretion of Glu into the small intestine lumen. The exocrine pancreas acinar cells not only avidly accumulate Gln but metabolize Gln to generate energy and to synthesize Glu for secretion in the pancreatic juice. Secreted Glu is suggested to play an important role during malnourishment in sustaining small intestinal homeostasis.

NEW & NOTEWORTHY Glutamine (Gln) has been suggested to have a trophic effect on exocrine pancreas and small intestine in malnourished states, but the mechanism is unknown. In this study, we suggest that this trophic effect derives from an interorgan relationship between exocrine pancreas and small intestine for Gln-glutamate (Glu) utilization involving the uptake and metabolism of Gln in acinar cells and secretion of Glu into the lumen of the small intestine.

acinar cells; enterocytes; glutamate dehydrogenase; glutaminase 2; SNAT5/Slc38a5

INTRODUCTION

Malnutrition is a highly prevalent and often overlooked complication in hospitalized patients. Studies have shown that between 20 and 40% of patients are malnourished or at nutritional risk (48). The state of malnutrition weighs heavily on clinical outcomes, significantly increasing both patient morbidity and mortality. Malnutrition can occur due to diseases but may be further exacerbated as a consequence of medical and surgical interventions. In a malnourished state, the body undergoes numerous physiological changes to cope with the increased stress presented by the reduced availability and quality of nutrients. Among the organs required to adapt are the exocrine pancreas and the small intestine, key organs for the digestion and absorption of nutrients. In malnourished animals and humans, the small intestine absorptive surface area is reduced due to decreases in cell proliferation, differentiation, and migration along the crypt-villi axis (41). In addition to morphological changes, the digestive activity decreases due to reduced functioning of the exocrine pancreas. Exocrine pancreas deficiency develops as a result of an insufficient amount or quality of protein arriving in the digestive tract, causing changes to the synthesis and secretion of digestive enzymes and a reduction in organ volume (7, 18, 29, 45). Even when adequate caloric content is supplied intravenously (total parenteral nutrition), morphological and functional alterations in the exocrine pancreas and small intestine are observed (3, 70). In these patients, further supplementing parenteral diets with glutamine (Gln) has a positive effect partially restoring the normal homeostasis of small intestine and pancreas (2, 24, 31).

Gln is the most abundant free amino acid in the plasma and the major carrier of nitrogen between organs. The Gln carbon footprint is found after mitochondrial metabolism to glutamate (Glu) and subsequently α-ketoglutarate (α-KG) in the anaplerosis of the tricarboxylic acid (TCA) cycle (71). Several enzyme classes participate in Gln and Glu metabolism. Glutaminase isoforms (GLS1 and GLS2) are responsible for deamidation of Gln to produce Glu and ammonia. Glu can also be synthesized from alanine (Ala) and aspartate (Asp). There are two isoforms of the alanine aminotranferases GPT1 and GPT2. GPTs catalyze the reversible transfer of an amino group from Ala to α-KG producing Glu and pyruvate. Aspartate aminotransferases (GOT) catalyze the reversible transfer of an amino group from Asp to α-KG producing Glu and oxaloacetate. Additionally, asparagine synthetase (ASNS) can synthesize Glu and asparagine from Gln and aspartate. Glutamate

Address for reprint requests and other correspondence: S. M. Camargo, Inst. of Physiology, Univ. of Zurich, Winterthurerstrasse 190, 8057 Zurich, Switzerland (e-mail: simonemc@physiol.uzh.ch).

dehydrogenase (Glud) further metabolizes Glu to α-KG, allowing it to enter the TCA cycle. In recent years, interest in targeting the Gln-Glu metabolism as a strategy to reduce cancer cell proliferation highlighted the plasticity and the importance of this metabolic axis (1). Gln transporters and metabolizing enzymes can be modulated to increase uptake and metabolism of Gln to generate energy, synthesize fatty acids, nucleotides, glutathione, and nonessential amino acids (8, 9, 21, 27, 34, 50, 53, 59, 67–69).

The Gln-Glu metabolism shows complex interorgan dynamics. While Gln is maintained at high plasma concentrations (~1 mM), Glu is maintained at low concentrations in extracellular fluids and high concentrations intracellularly (62). In healthy subjects, the plasma Gln pool is mostly the result of intestinal absorption as well as being released from skeletal muscle, lungs, and adipose tissue (5, 32). Glu, which is found in high concentrations in ingested proteins, is efficiently absorbed as a free amino acid and in peptides by enterocytes and is predominantly metabolized to neutral amino acids and α-KG and used locally as a principal source of energy (12, 46, 52, 61, 65). The plasma Gln pool is used by the kidneys to produce ammonia, which is further metabolized by the liver to urea, thus controlling the nitrogen balance in the body (19). The brain avidly takes up Gln and additionally synthesizes it from Glu. Astrocytes metabolize the Glu released by the neurons to Gln, maintaining high Gln and low Glu concentrations in the brain interstitial fluid (20, 64). In the endocrine pancreas, the synthesis of Glu in β-cell mitochondria was shown to enhance glucose-stimulated insulin secretion (28, 33, 43), suggesting a link between metabolism of Glu and glucose homeostasis (44, 49). Gln accumulates rapidly in the pancreatic acinar cells (14, 51) due to the expression of basolateral membrane amino acid transporters that can actively accumulate Gln and other neutral amino acids (55). Glu is transported by the sodium-dependent Slc1 family members, also known as the excitatory amino acid transporters (EAATs). The sodium-independent exchanger xCT (Slc7a11) is reputed to efflux Glu from cells. In the small intestine, luminal Glu was shown to be the most important energy source (4, 65, 66). Stoll and Van der Schoor (61, 63) demonstrated that in enterocytes 36% of the energy utilized was gained from luminal Glu and only 15% from arterial Gln. Glu does not reach the lumen of the small intestine solely though ingested foods; additionally, the basal secretion of the exocrine pancreas is rich in Glu (25), suggesting that Glu secreted by the pancreas may be reabsorbed by the small intestine. Despite Gln and Glu seeming to play critical roles in the function of the pancreas and small intestine, their transport and metabolism are not fully understood. Additionally, the role of Glu secreted by the exocrine pancreas into the lumen of the small intestine has not yet been addressed. In the present study, we first investigated the pancreatic origin of Glu, its accumulation in cells including the transporters and enzymes involved, as well as its release into the small intestine as a result of stimuli. Second, we analyzed the effect of protein diet restriction on pancreatic Glu secretion and intestinal Glu transport and metabolism.

METHODS

Animals and diets. Mice (C57Bl/6J) and rats (Wistar) were housed in standard conditions and fed a standard diet. Animals were then either kept on a standard diet (20%), or switched to a protein-deficient diet (0% casein added) or high-protein diet (40% casein). The modified standard diet AIN93G was maintained isocaloric by adjusting the starch content (Kliba-Nafg, Kaiseraugust, Switzerland). Mice or rats housed in groups (3–4 per cage) were fed experimental diet for 8–12 days (8–10 days for mice and 9–12 days for rats). Animals were weighed daily, and experiments were always run at the same time to minimize circadian variations. All procedures for animal handling were according to the Swiss Animal Welfare laws and approved by the Kantonales Veterinäramt Zürich.

Amino acid quantification by ultra-performance liquid chromatography. The analysis was performed at the Functional Genomics Center Zurich. Samples were deproteinized with sulfosalicylic acid (5% final concentration), and amino acid concentrations were determined using the MassTrak (pancreatic juice, plasma) or AccQTag (cell culture) Amino Acid Analysis Solution method (Waters, Milford, MA) according to the manufacturer's instructions.

Protein and DNA measurements. Protein content was measured by a modified Lowry method (Bio-Rad, Hercules, CA) and DNA using fluorescence quantitation kit (Sigma-Aldrich, St. Louis, MO) according to the manufacturer's instructions.

Pancreatic juice collection. Pancreatic juice collection was performed as described before (29). Briefly, rats were starved for 12 h and anesthetized with isoflurane, the pancreatic duct was localized, and the upper right loop of the duodenum was fixed. The biliary duct was cannulated and deviated to the lumen of the small intestine with a small incision on the wall. The pancreatic duct proximal to the sphincter of Oddi was cannulated with polythene tube (0.4-mm inner diameter and 0.8-mm outer diameter). Pancreatic juice was collected on ice. At the end of the collection, heart blood was collected and a higher dose of isoflurane was applied to euthanize animals. Every day pancreatic juice of three rats, one each diet, was collected. For experiments where the effect of cholecystokinin peptide CCK-8 and secretin was analyzed, a jugular catheter (blunt PE50) was used. Prewarmed saline infusion at 1 ml/h was maintained constant. Bolus (0.5–1 ml) of secretin (Bachem, Bubendorf, Switzerland) at a dose of 3 pmol/100 g and the cholecystokinin peptide CCK-8 (Bachem) at 125 pmol/100 g was used. In this experiment, pancreatic juice was collected every 15 min and the volume and protein content were measured. For the ultra-performance liquid chromatography measurement, samples were pooled. For the basal phase, all four samples were pooled. After CCK-8 treatment, the two samples with the highest protein content were pooled, whereas after secretin injection, the two samples with highest volume were pooled.

RNA extraction and real-time quantitative PCR. RNA was extracted with RNeasy kit (Qiagen, Venlo, The Netherlands). Approximately 2 mm^3 of frozen pancreas were homogenized with MagNa Lyser Green Beads (Roche, Basel, Switzerland) for 1 min (2 × 30 s, 6,000 rpm) or for cells ~1×10^5 AR42J cells were homogenized by passing through a 20-gauge needle. RNA quantity was analyzed by ND-1000 NanoDrop UV-spectrophotometer (NanoDrop Technologies Wilmington, DE). RNA quality was analyzed by microchip analysis Agilent 2100 Bioanalyzer (NanoChip; Agilent Technologies, Santa Clara, CA). Total RNA (20 ng/μl reaction) was used as template for reverse transcription with the TaqMan Reverse Transcription Kit (Applied Biosystems, Foster City, CA) according to the distributer. Quantitative PCR (qPCR) was performed using 10 ng of pancreatic or small intestine cDNA as a template. The reaction was carried out with the Taq-Man Universal PCR master mix (Applied Biosystems) using a Prism 7700 cycler (Applied Biosystems). The abundance of the target messenger RNAs was calculated relative to a housekeeping gene [hypoxanthine phosphoribosyltransferase (HPRT)] or 18S ribosomal RNA (18S) and expressed as relative expression ($R = 2^{[Ct(housekeeping\ gene) - Ct(test)]}$), where Ct is the cycle number observed at the threshold. Primers that have not yet been published (11, 38, 42, 55) are listed in Table 1.

Acinar cell isolation. Pancreata from mice or rats were excised, washed in cold HBSS (calcium and magnesium free), freed from fat

Table 1. *Primers and probes used for quantitative PCR mouse and rat genes*

Gene	Species	Primers*	Universal Probe Library Roche	Accession No.
Gls1	Mouse			
Sense		AAGCAGTCTGGAGGGAAGGT	73	NM_001081081.2
Antisense		ACACCCCACAAATCAGGACT		
Gls2	Mouse			
Sense		GTATGACTTCTCGGGCCAGT	97	NM_001033264.3
Antisense		TCCTGACACAGCTGACTTGG		
Glul	Mouse			
Sense		GGTTGGAATGGAGCAGGAATA	97	NM_008131
Antisense		GCTCCCACACCGCAGTAA		
Gpt1	Mouse			
Sense		GCCGTCCTTCAAGCAGTTT	34	NM_182805.2
Antisense		GCTCCGTGAGTTTAGCCTTG		
Gpt2	Mouse			
Sense		CGTGGAGGCAGCTCAGTC	25	NM_173866.3
Antisense		GCCAGGCACGACACAGAT		
Got1	Mouse			
Sense		TTCAGTTTCACCGGCTTGA	51	NM_010324.2
Antisense		AGCCGCACATGTTGATCC		
Got2	Mouse			
Sense		ATCGAGCAGGGCATCAAT	34	NM_010325.2
Antisense		TTGCAGACCACCGTGAAG		
Glud	Mouse			
Sense		TCCTGGAAAGAAACATCATGG	25	NM_008133.4
Antisense		TTTAGCCACTCAAAGTAAGACACTG		
Bcat2	Mouse			
Sense		GACAGGATGCTACGTTCTGCT	17	NM_009737.3
Antisense		ATGAGCTGGCGGATACACTC		
Asns	Mouse			
Sense		CCAACCGGTCTTGTCACTG	34	NM_012055.3
Antisense		CACATGCTACAGGCGGACT		
Caspase 3	Mouse			
Sense		TCTTACTGAAGACATTTTGGA	9	ENSMUST00000093517
Antisense		AGGCCCATTTGTCCCATA		
Cdk2	Mouse			
Sense		CTGCATCTTTGCTGAAATGG	80	NM_016756.4
Antisense		GATCCGGAAGAGTTGGTCAAT		
Ccne2/cyclinE2	Mouse			
Sense		GCCATCGACTCTTTAGAATTT	71	NM_001037134.1
Antisense		TGTCATCCCATTCCAAACCT		
Ccnd1/cyclinD1	Mouse			
Sense		AGAAGGAGATTGTGCCATCC	67	NM_007631.2
Antisense		CTCTTCGCACTTCTGCTCCT		
Cdkn1b/P27/kip	Mouse			
Sense		GTTAGCGGAGCAGTGTCCA	62	NM_009875.4
Antisense		TCTGTTCTGTTGGCCCTTTT		
Muc2/Mucin 2	Mouse			
Sense		ACCTCCAGGTTCAACACCAG	10	NM_023566.3
Antisense		GTTGGCCCTGTTGTGGTC		
Gls1	Rat			
Sense		GATAAACCACATAATCCGATGGT	67	ENSRNOT00000068091.1
Antisense		TTCTCAGCATTATTTACTCCTTGC		
Gls2	Rat			
Sense		GTATGACTTCTCGGGCCAGT	97	ENSRNOT00000018737.4
Antisense		TTGGGTACAACCAGGAGGAT		
Glud1	Rat			
Sense		CAGAGGCCGATAAGATTTTCC	25	ENSRNOT00000013788.3
Antisense		TGATTTAGATTCTTTAGCCACTCAAA		
Got1	Rat			
Sense		ACCGACCCAACTGAAGAGG	38	ENSRNOT00000022309.5
Antisense		TGAGTCAAAGAAGGGGAACAG		
Got2	Rat			
Sense		GCGTCGGTAGTGAAGAAAAGAC	9	ENSRNOT00000006466.3
Antisense		GCATGGTCCAGGAGTCCTTA		
Gpt1	Rat			
Sense		TTCGAGGACCCATTGTGC	17	ENSRNOT00000050556.2
Antisense		TCAGTAAACGGCTTCTTCACAC		
Gpt2	Rat			
Sense		GAGGTAATCCGAGCCAACAT	105	ENSRNOT00000022851.4
Antisense		GGTAGGTGCAGAGAGCCATC		

Continued

Table 1.—*Continued*

Gene	Species	Primers*	Universal Probe Library Roche	Accession No.
Slc1a3/EAAT1	Rat			
Sense		CTGGCCAAGAAGAAAGTTCAG	9	NM_019225.1
Antisense		GCAAATCCAAGGATTGTACCC		
Slc38a5/SNAT5	Rat			
Sense		ACCCTCACTGTGCCTGTTGT	67	NM_138854.1
Antisense		TGAAGGCCTTACTTGGGAAG		
Slc1a4/ASCT1	Rat			
Sense		CTGGGGCTGGAGAACTCA	25	NM_198763.1
Antisense		GGAAGGGAACAGGTTTCTGA		
Slc7a11/xCT	Rat			
Sense		GGTTGCCCTTGGCTTTTTAT	20	NM_001107673.2
Antisense		TTTTCAGGGTTGTCTACTTCTTCA		
Slc7a5/LAT1	Rat			
Sense		GGGTCTCTGTTCACGTCCTC	97	NM_017353.1
Antisense		AGAAGCTGTGGGTGGATCAT		

*The primers and probe pairs were designed using an universal library software, and probes were purchased from Roche (Basel, Switzerland).

and mesenteric tissue, rapidly cut with scalpel, and added to the digestion medium. The tissue was incubated for 20 min in 10 units collagenase NB8 (Serva, Heidelberg, Germany) in HBSS supplemented with 0.1 mg/ml trypsin inhibitor, 8.7 mM $CaCl_2$, and 25 mM HEPES pH 7.4. The digestion was stopped by addition of 50 ml of cold HBSS supplemented with 5 mg/ml BSA and 22 mM HEPES pH 7.4. For RNA extractions, the cell suspension was subsequently filtered using 100- and 40-μm nylon cells strainers (Corning, New York, NY). The pellet was washed in cold HBSS and snap frozen. For uptake studies, acini were washed and resuspended in cold BSA-Krebs-Tris solution (1 mg/ml BSA, 118 mM NaCl, 4.7 mM KCl, 1.2 mM KH_2PO_4, 1.2 mM $MgCl_2$, 1.25 mM $CaCl_2$, and 20 mM HEPES pH 7.4). For secretion experiments, only the 100-μm strainer was used and acini were washed and resuspended in cold extracellular solution supplemented with 1 mg/ml BSA (140 mM NaCl, 5 mM KCl, 2 mM $NaHCO_3$, 1 mM NaH_2PO_4, 1.2 mM $MgCl_2$, 1.5 mM $CaCl_2$, 3 mM glucose, and 10 mM HEPES, pH 7.4).

Gln, glucose, leucine, and palmitoyl oxidation rates and uptake of Gln in freshly isolated acini. Uniformly labeled [U-^{14}C]glucose (300 mCi/mmol), [U-^{14}C]Gln (200 mCi/mmol), [U-^{14}C]leucine (329 mCi/mmol), and [1-^{14}C]palmitoyl (60 mCi/mmol) (Hartmann Analytic, Braunschweig, Germany) were added to a final concentration of 5 mCi/ml in 1 mM (with the exception of palmitoyl) unlabeled substrate to freshly isolated acini in 2-ml tubes. Inside the 2-ml tube, a 0.2-ml tube without cap, containing 100 μl trap solution (0.1 M KOH), was carefully added and the 2-ml tube was sealed with Parafilm in an air-tight manner. The tube was incubated at 37°C for 90 min under agitation (110 rpm). Following incubation, tubes were kept for 10 min on ice and opened carefully and 90 μl KOH solution were added to the scintillation cocktail for the measurement of carbon dioxide formation (CO_2). Cells were washed and used for DNA quantification. The data are expressed as nanomoles per CO_2 per hour per micrograms of DNA. Freshly isolated acini were also used for measuring the uptake of Gln. Cells were incubated for 5 min at 37°C in Krebs-Tris buffer containing 1 mM and 0.1 μCi/ml tritiated substrate. After being washed, cells were used to determine the uptake by liquid scintillation counting and for the measurement of protein and DNA content. Gln transport is expressed as nanomoles substrate per 5 min per micrograms of DNA. The protein and DNA measurements were also performed to estimate protein synthesis in acinar cells of mice under different diets (mg total protein/μg DNA).

Secretion of Glu in freshly isolated acini. Freshly isolated acini were allowed to recover for 90 min in a cell culture incubator (37°C, 5% CO_2) with extracellular medium supplemented with 1 mg/ml BSA, 0.1 mg/ml trypsin inhibitor, and 2 mM Gln in the absence or presence of 6-diazo-5-oxo-L-norleucine (DON; 250 μM). The acini were washed, divided in 2-ml tubes, and resuspended in 1 ml of a solution containing BSA (1 mg/ml) (control) and 2 mM Gln, leucine, or alanine. For the acini treated with DON during the recovery, the secretion solutions were also supplemented with 250 μM of the glutaminase inhibitor DON. After a 1-h incubation at 37°C with agitation (100 rpm), tubes were spun (100 *g*) and the upper 500 μl of supernatant were collected. The cells were washed in cold extracellular medium and lysed in water and protease inhibitor. Glu secreted in the medium and in the cells was measured with the Amplex Red glutamic Acid/Glutamate Oxidase Assay Kit (Molecular Probes, Eugene, OR). The results are expressed as nanomoles Glu per micrograms of DNA.

AR42J culture for amino acid analysis and uptakes. AR42J cells (CRL-1492; ATCC) were cultured as described by Sonda et al. (60), with F-12K Nut Mix Medium (GIBCO) supplemented with 20% fetal calf serum (FCS). For uptake experiments, 0.1×10^6 cells per 3.8 cm^2 were plated and cultured for 6 days, followed by treatment with 50 nM dexamethasone for 24 h to induce differentiation. Afterwards, cells were incubated for 24 h in F-12K Nut Mix Medium-FCS in the absence or presence of 250 μM of DON, L-cycloserine (CySer), or aminooxy-acetic acid hemihydrochloride (AOA; Sigma-Aldrich). For ultra-performance liquid chromatography measurements, cells were washed with PBS and lysed with 100 μl ice-cold water containing protein inhibitor cocktail (2 μl/ml) (Sigma-Aldrich). For uptake measurements, cells were washed with amino acid free high glucose DMEM (Invitrogen, Basel, Switzerland). DMEM containing glucose (25 mM), Gln, or Glu and 0.1 μCi/ml of tritiated compounds (Hartmann Analytic) was used for 2 min uptakes at 37°C. After cells were washed with cold PBS, 120 μl of 1% SDS in water were used to scrape and sonicate cells. The lysate was used to determine uptake by liquid scintillation counting and normalization to DNA content. Transport is expressed as nanomoles per 2 min per micrograms of DNA.

Isolation of acinar cell zymogen granule vesicles. Mouse pancreata were weighed and homogenized in 0.3 M sucrose (2 mM MOPS, pH 6.8, 1 mM EDTA, 0.5 mM PMSF, 10 μg/ml aprotinin, and 5 μg/ml pepstatin) using a Teflon pestle PYREX Potter-Elvehjem tissue grinder powered by a variable-speed rotary drill for nine strokes at 3,000 rpm. The homogenate was centrifuged 10 min at 750 *g* at 4°C, and the supernatant was filtered through a 20-μm nylon mesh (Millipore, Bedford, MA). The filtered extracts were centrifuged at 1,750 *g* for 20 min at 4°C, and pellets were resuspended in 1 ml homogenization buffer and further purified by separation with an equal volume of Percoll gradient [60% vol/vol Percoll (Amersham Biosciences, Piscataway, NJ), 0.28 M sucrose, 20 mM MOPS pH 6.8, 1 mM EDTA, 0.5 mM PMSF, 10 μg/ml aprotinin, and 5 μg/ml pepstatin]. After 30 min centrifugation at 60,000 *g* at 4°C, the white zymogen granule layer near the bottom of the tube was collected and washed.

The quality of the freshly isolated zymogen granule vesicles (ZGVs) was verified by transmission electron microscopy (TEM). ZGVs were subsequently used for surface biotinylation and amino acid measurements. Zymogen granules and total pancreas were lysed in water containing protease inhibitor cocktail (2 μg/ml) and used for amino acid and protein measurements. The results are expressed as nanomoles of amino acid per milligrams of protein.

Preparation of ZGVs for TEM. Isolated ZGVs were fixed in glutaraldehyde at 4°C, washed, and treated with 1% OsO_4 for 1 h, embedded with 2% agar, and dehydrated. Epon blocks were cut at a thickness of 70 nm and treated with 2% uranyl acetate and lead citrate. The slides were analyzed at the Center for Microscopy and Image Analysis of the University of Zurich using a TEM Philips CM100 (1994, 40–100 kV). Pictures were taken at ×17,500 magnification.

Surface biotinylation of ZGVs. After purification, fresh ZGVs were incubated with 1 mM 2-aminoethyl)methanethiosulfonate hydrobromide (MTSEA-biotin; Sigma-Aldrich) for 30 min at 4°C. The biotinylated ZGVs were washed, lysed, and incubated with immobilized streptavidin agarose resin beads (Pierce, Rockford, IL) for 2 h at room temperature. The beads were washed (50 mM Tris·HCl pH 7.4, 100 mM NaCl, and 5 mM EDTA), and protein was eluted with 50 μl of 2× sample buffer with 5% β-mercaptoethanol and heated for 15 min at 65°C. Proteins were separated on polyacrylamide gel (8 or 10%) and transferred electrophoretically to PVDF membranes (Immobilon-P; Millipore). Total membrane lysate or crude synaptosomes were used as positive controls for each antibody as described in the respective figure legends. Membranes were incubated overnight at 4°C with Rab3D (Abcam, Cambridge, UK), EAAT1 (Santa Cruz Biotechnology, Dallas, TX), EAAT3 (Alpha Diagnostics, San Antonio, TX), and vGLUT3 (1:1,000; SYSY, Göttingen, Germany). Appropriate horseradish peroxidase-conjugated secondary antibodies (1:5,000; Promega, Madison, WI) and Luminata horseradish peroxidase chemiluminescent substrate (Millipore) were used for chemiluminescent detection using the luminescent image analyzer LAS-4000 (Fujifilm).

Everted intestinal ring uptake of Glu and leucine. Uptake of radiolabeled amino acids was performed by the previously described methods that were modified to eliminate mucus (13, 35, 39). Briefly, the small intestine was removed from ~2 cm distal to the stomach and 1 cm proximal to the cecum. The proximal (jejunum) and distal (ileum) segments were washed with 50 ml of Na-free Krebs-Tris solution (with 100 mM NMDG substituted for NaCl) to remove secretions and remainder of digested food. Further washes with 25 ml DEAE (1.25g/25 ml soaked overnight), 75 units/ml heparin, and 1 mM DTT and Na-free solution at room temperature were performed. The length and weight of the segments were measured. Segments were everted and cut in ~1-cm rings. For uptakes, rings were incubated in prewarmed, oxygenated (Oxycarbon) Krebs-Tris buffer (pH 7.4) containing 0.01 or 1 mM Glu and 1 mM leucine (0.1 μCi [^{3}H]/ml) for 1 min at 37°C. After rings were washed with ice-cold buffer, they were weighed and lysed with Solvable (Perkim Elmer, Waltham, MA) and the radioactivity was determined by liquid scintillation counting. Transport is expressed as picomoles of amino acids per minute per milligrams of wet tissue.

Sample preparation and Western blot analysis. Crude pancreatic and small intestinal membranes from mice treated with diets containing 0 or 40% casein were prepared as described previously (55). The pancreatic and small intestine crude membranes (25 or 50 μg) were immunoblotted as previously described and membranes incubated with primary antibodies. Antibodies against glutaminase 2 (Prosci, Poway, CA), GPT1 (Abcam), Glud (Cell Signaling, Danvers, MA), B^0AT1 (Pineda, Berlin, Germany), and EAAT3 (Alpha Diagnostics) were diluted to 1:1,000. Zonula occludens-1 (ZO-1) and occludin (Zymed, San Francisco, CA) were diluted 1:500. Mouse monoclonal anti-actin (Sigma) signal was used to normalize the signals from pancreatic samples, and mouse monoclonal anti-NaKATPase (Santa Cruz Biotechnology) was used for normalization of small intestine sample signals. Quantification of bands was performed using the free software ImageJ (https://rsbweb.nih.gov/ij/index.html).

Immunofluorescence and morphological analysis. Both paraffin and cryosections were used. Mouse pancreas and rat small intestine tissue samples were fixed in 3% paraformaldehyde. After fixation small intestine tissue was prepared as paraffin blocks and the pancreatic tissue as cryoblocks, as previously described (55). Sections of paraffin and cryosections (5- and 9-μm thickness, respectively) were used for immunofluorescence and hematoxylin-eosin staining. Sections were incubated with primary antibodies (diluted in PBS, 2% BSA, and 0.04% Triton X-100) overnight at 4°C, with the exception of sections treated with the Ki67 antibody, which were incubated for 30 min at room temperature. Subsequently, sections were incubated with the appropriate secondary antibodies (Table 2) and mounted in Glycergel (DakoCytomation, Glostrup, Denmark). The hematoxylin-eosin staining was carried out using a standard protocol as described elsewhere (60). Sections were viewed on a Nikon Eclipse TE300 epifluorescence microscope (Nikon Instruments, Melville, NY) equipped with a DS-5M Standard charge-coupled device camera (Nikon Instruments) and acquired with NISElements (Nikon Instruments). Images were merged using Photoshop 9. The poststaining analyses of images for crypt and villi measurements and quantification of Ki67-positive cells were done using the Imaris software (Bitplane, South Windsor, CA).

Statistics. Pooled data are shown as means ± SE (n), where n represents the number of independent observations. For statistical comparison, ANOVA followed by Bonferroni posttest or two-tailed t-test were performed using a statistical software package (Prism v. 4.0; GraphPad, San Diego, CA).

Table 2. *Antibodies and conditions used for immunofluorescence*

Antigen	Primary Antibody/Cell Marker	Dilution	Antigen Retrieval	Secondary Antibody (Molecular Probes)
EAAT1	Santa Cruz Biotechnology	1:100	Cryosection, 0.1% SDS in PBS (5 min/room temperature).	Alexa Fluor 488 donkey-anti-rabbit IgG (1:500) Alexa Fluor 594 donkey-anti-rabbit IgG (1:500)
EAAT3	Alpha Diagnostics	1:1,000	Paraffin, Na-EDTA pH 8 (5 min/98°C)	Alexa Fluor 488 goat-anti-rabbit IgG (1:500)
B^0AT1	MVRLVLPNPGLEERIC Pineda	1:200	Paraffin, Na-EDTA pH 8 (5 min/98°C)	Alexa Fluor 568 goat anti-guinea pig IgG (1:500)
Ki67	Dako	1:25	Paraffin, 10 mM Na-citrate pH 6 (20 min/98°C)	Alexa Fluor 594 donkey-anti-mouse IgG (1:500)
DNA	DAPI, Merck	1:5,000		—
Actin	Texas Red-X Phalloidin, Molecular Probes	1:100		—
PNA	FITC-PNA, Vector	1:250		—

EAATT, excitatory amino acid transporter; PNA, peanut agglutinin.

RESULTS

Acinar cells secrete Glu in pancreatic juice during constitutive and stimulated secretion. Glu showed the highest accumulation in pancreatic juice in comparison to plasma levels. In constitutively secreted pancreatic juice of unstimulated anesthetized rats the concentration of Glu was approximately sixfold higher than in plasma, whereas the concentration of all other amino acids, but aspartate, was clearly lower than in plasma (Fig. 1*A*). To evaluate if hormonal stimulation of acinar and ductal cells influences the secretion of Glu in pancreatic juice, Glu concentration was measured before (basal) and after stimulation with cholecystokinin (CCK-8; acinar cells) and secretin (ductal cells). Effective stimulation of acinar cells by CCK was evaluated by measuring protein secretion. Ductal stimulation was confirmed by the increased fluid volume observed after secretin treatment (Fig. 1*B*). CCK stimulated not only protein release from ZGVs but also induced a significant increase in the secretion of free Glu. However, the additional stimulation of ductal cells with secretin did not further increase Glu secretion. These data demonstrate that Glu is constitutively secreted by acinar cells and acinar cell stimulation induces increased Glu secretion, while stimulation of ducts does not influence Glu secretion in pancreatic juice.

Glu accumulation in acinar cells is not the result of Glu transport. We analyzed the expression of Glu and Gln transporters in freshly isolated acini and in the acinar cell line AR42J. The Glu secreted into pancreatic juice may result from its accumulation in acinar cells due to import from the extracellular space or metabolism. As previously described for total mouse pancreas (55), Glu transporters were found to have a low gene expression relative to housekeeping genes also in isolated rat acini and AR42J cells (Fig. 2*A*). Neutral amino acids can be transported into acinar cells by the sodium-dependent Gln and the neutral amino acid transporters SNAT3 (Slc38a3) and SNAT5 (Slc38a5) and the sodium-independent exchangers LAT1-4F2 (Slc7a5-Slc3a2) and LAT2-4F2 (Slc7a8-Slc3a2), which are localized at the basolateral membrane of acinar cells. In freshly isolated acini and AR42J cells, the expression of Glu transporters of the Slc1 and Slc7 families and Gln transporters of the Slc38, Slc1, and Slc7 families displayed similar expression patterns (Fig. 2*A*). Functionally, the accumulation of radiolabeled amino acids measured in freshly isolated acini and AR42J cells showed that Glu uptake was up to sixfold lower than that of Gln (Fig. 2, *B* and *C*), supporting the hypothesis that accumulation of Glu in pancreatic juice is not primarily due to Glu transport.

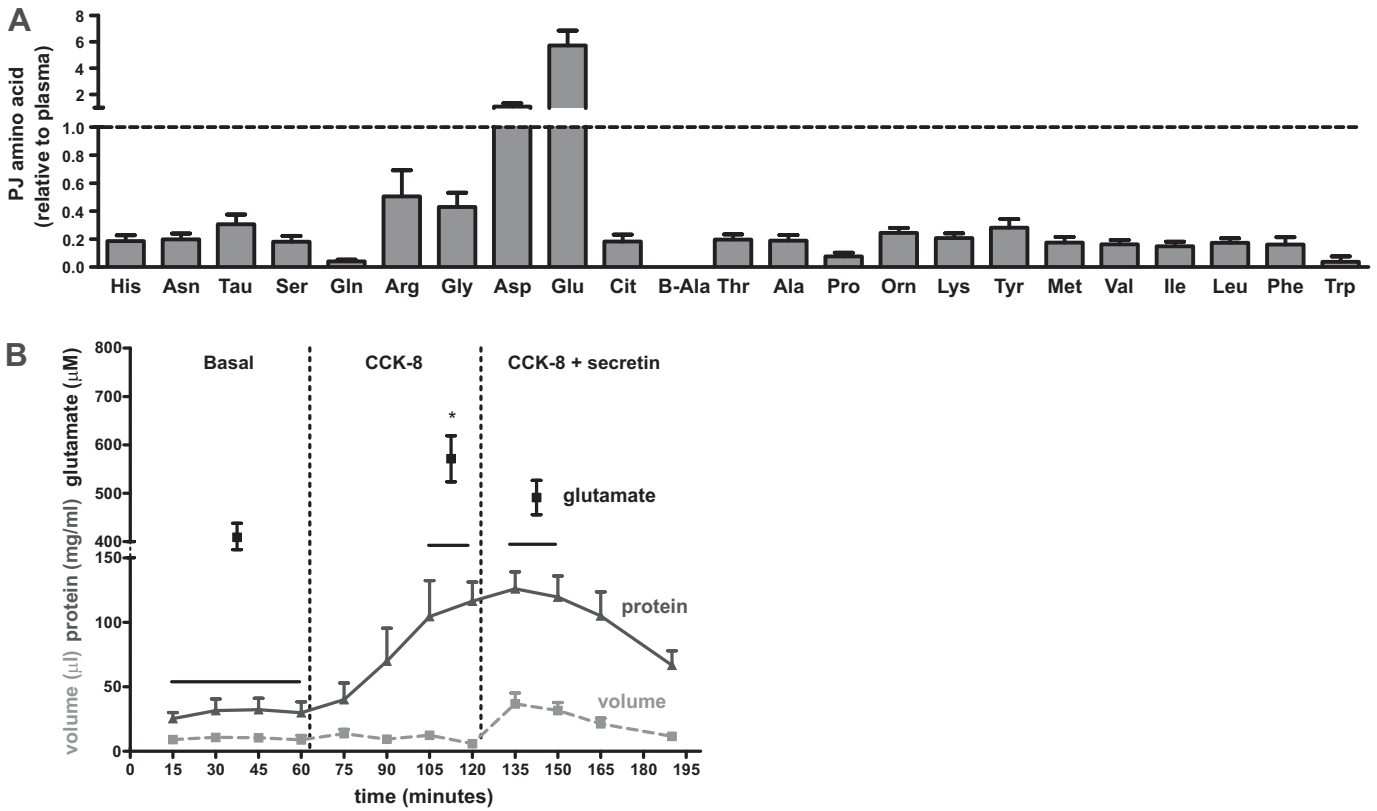

Fig. 1. Glutamate is secreted in pancreatic juice (PJ) by acinar cells during constitutive and stimulated secretion. *A*: glutamate secretion in unstimulated rats. The ratio of amino acid in PJ to plasma was calculated from samples of rats fed normal-protein diet. Amino acid concentrations were analyzed by ultra-performance liquid chromatography (UPLC), and the raw data are depicted in the Fig. 5, *E* and *F*. Results are expressed as means ± SE; $n = 7$ rats. *B*: glutamate secretion is increased by acinar cell stimulation. After basal collection of pancreatic juice every 15 min, animals received a bolus injection of CCK-8 (2.5 nmol/kg) at 60 min, followed by the cholecystokinin peptide CCK-8 + secretin (2.5 nmol/kg + 30 pmol/kg) at 120 min. Glutamate concentration was analyzed by UPLC (black squares). Protein (dark gray triangle, dashed line) and volume (light gray squares, solid line) were measured as described in METHODS. Results are given as means ± SE; $n = 5$ rats. *$P < 0.05$ (ANOVA with post hoc Bonferroni test).

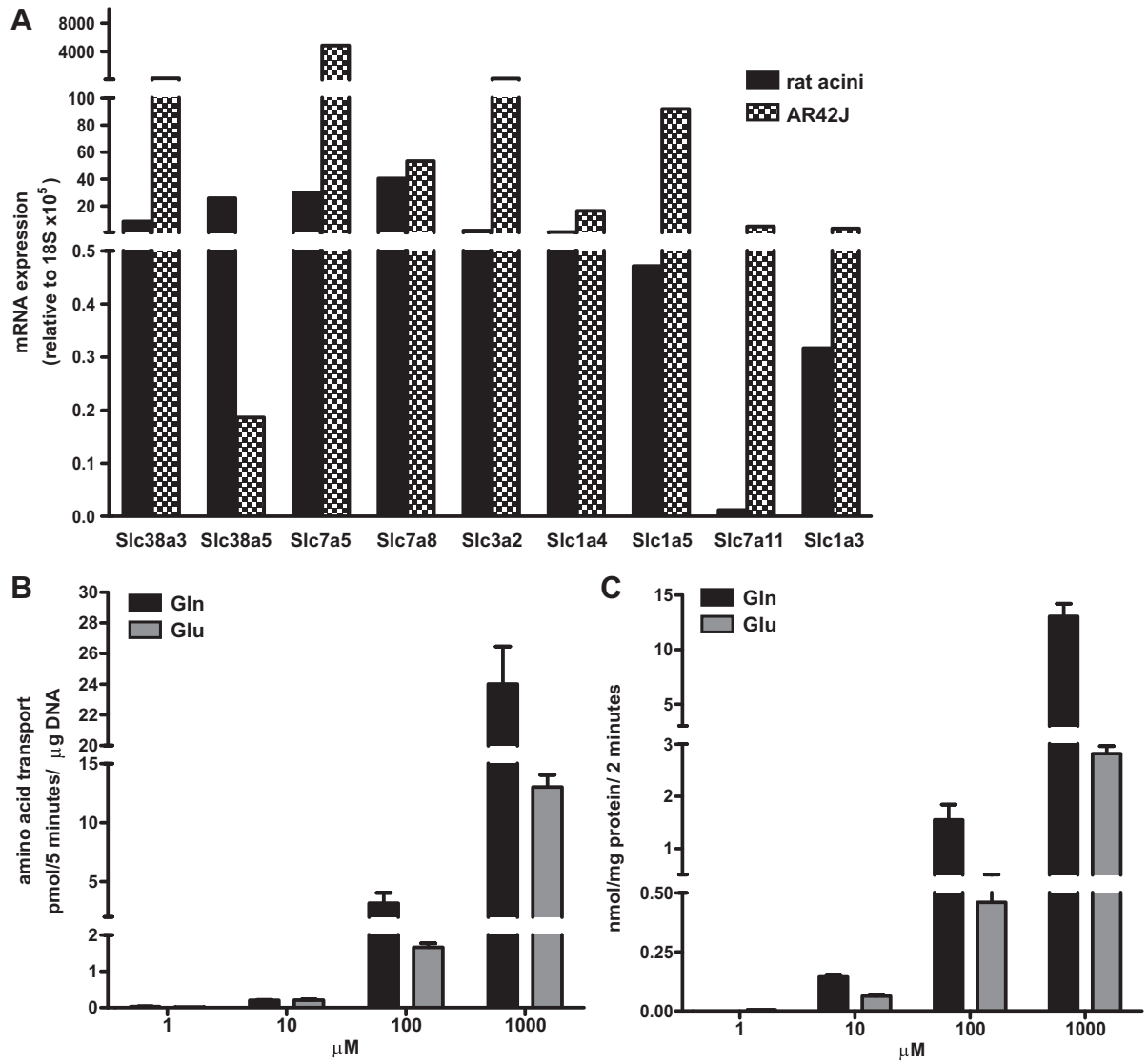

Fig. 2. Glutamine (Gln), but not glutamate (Glu), is efficiently accumulated in acinar cells. *A*: Glu and Gln transporter mRNA expression in freshly isolated rat acinar cells and AR42J. mRNAs expression of the Gln and neutral amino acid transporters slc38a3/SNAT3, slc38a5/SNAT5, slc7a5/LAT1, slc7a8/LAT2, slc3a2/4F2hc (accessory protein), slc1a4/ASCT1, and slc1a5/ASCT2 and of the Glu transporters slc7a11/xCT and slac1a3/excitatory amino acid transporter 1 (EAAT1) in freshly isolated rat acinar cells (black bars) and AR42J cells (hatched bars). Values are expressed relative to 18S RNA. *B* and *C*: Gln and Glu transport in freshly isolated acinar cells (*B*) and AR42J (*C*). *B*: freshly isolated mice acinar cells were incubated with Gln or Glu (1, 10, 100, and 1,000 μM) for 5 min at 37°C. The results are expressed as pmol·5 min^{-1}·μg DNA^{-1} and are reported as means ± SE; $n = 4$ mice. *C*: AR42J cells were used for uptake of Gln (10, 100, and 1,000 μM, black bars) or Glu (1, 10, 100, and 1,000 μM, gray bars) for 2 min at 37°C. The results (means ± SE) are expressed as nmol·2 min^{-1}·mg $protein^{-1}$; $n = 3$ wells per concentration.

Acinar cells metabolize Gln to synthesize Glu. Gln, which is highly accumulated in acinar cells, proved to be the favored substrate for energy production in these cells. The amount of carbon dioxide (CO_2) formed from Gln in freshly isolated acini was higher than the amount formed from glucose, palmitoyl or leucine (Leu) (Fig. 3*A*). Before entering the TCA cycle, Gln is metabolized to Glu, suggesting a high Gln to Glu metabolism in these cells. As shown in Fig. 3*B*, transcripts for both isoforms of glutaminase (GLS1 and GLS2) were present in acinar cells. The cytosolic and mitochondrial isoforms of the alanine (GPT1 and GPT2) and aspartate (GOT1 and GOT2) aminotranferases, and Glud were also expressed. The enzyme responsible for Gln synthesis from Glu, glutamine synthase (Glul) is also expressed in acinar cells (Fig. 3*B*). Although in isolated acini the expression of all the aforementioned enzymes was lower than in cultured cells, the relative expression patterns were similar. Additionally, AR42J differentiation is induced by dexamethasone, which is a known inducer of Glul expression (17) and may also increase the expression of other enzymes. To verify the participation of these enzymes in the synthesis of Glu, we pharmacologically inhibited GLS, GPT, and GOT in AR42J cells and measured the accumulation of Glu, Gln, Ala, and Asp. As depicted in Fig. 3*C*, inhibition of the glutaminases using DON significantly increased Gln and reduced Glu concentrations. The alanine aminotransferase inhibitor CySer induced only a nonstatistically significant reduction in Glu and Ala concentrations. The inhibition of aspartate aminotransferase using AOA did not change Glu or Asp

concentrations (Fig. 3*C*). Since DON is structurally similar to Gln, we checked if it indirectly reduced Glu accumulation by competitively inhibiting transport (and therefore availability) of enzyme substrates. In the presence of DON, Gln, Glu, and glucose transport were not changed (Fig. 3*D*), supporting the conclusion that changes in intracellular Gln/Glu ratios were due to glutaminase inhibition. We also studied the accumulation and secretion of Glu in freshly isolated acinar cells. Gln addition to the incubation medium induced Glu secretion and increased cellular Glu accumulation. In the presence of DON, both the accumulation and secretion of Glu were reduced (Fig. 3*E*). We observed that cells supplemented with Ala also secreted and accumulated more Glu in the cells than the control, suggesting a role for GPT in Glu synthesis. Con-

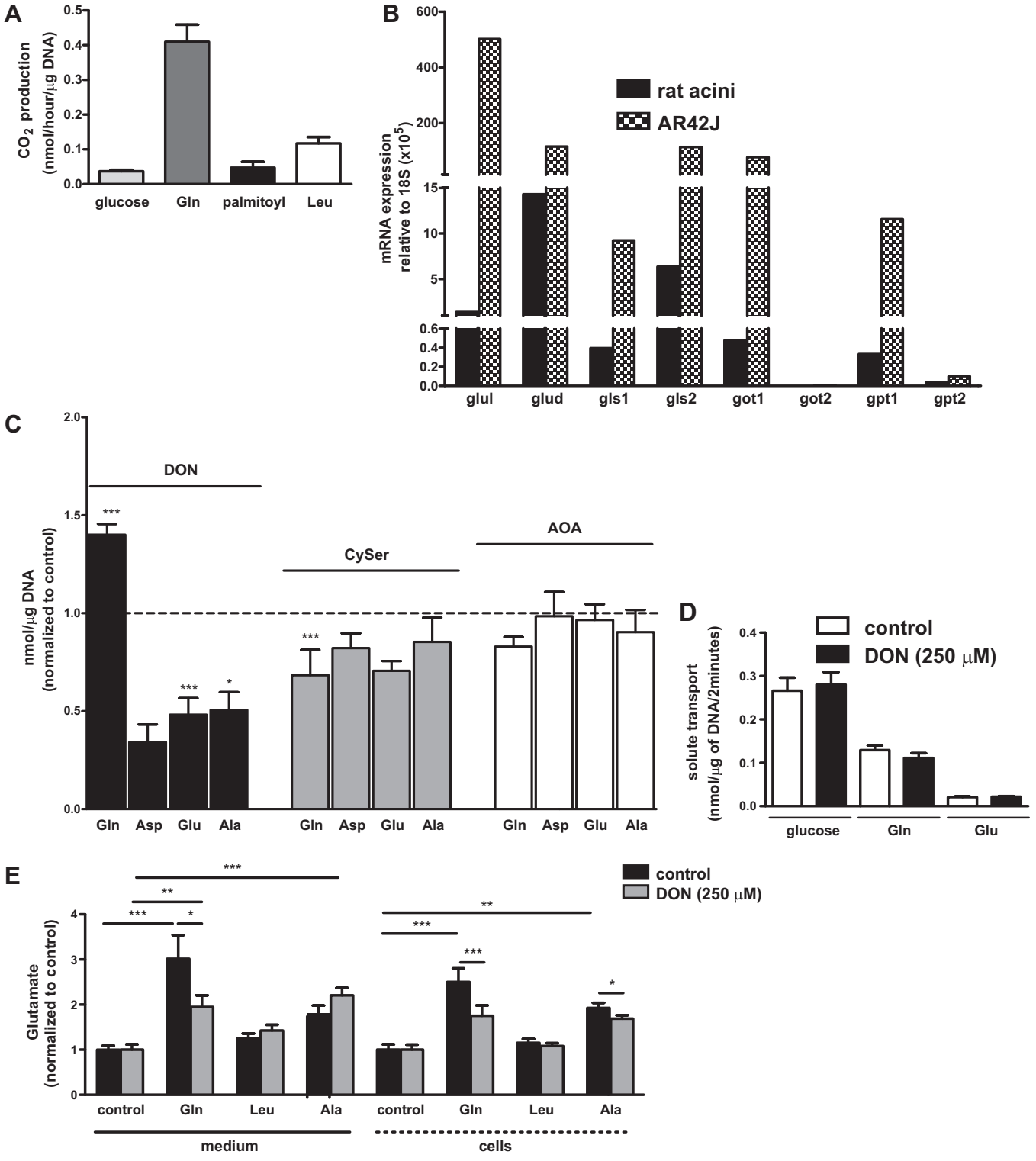

versely, addition of Leu did not cause significant changes in cell content and secretion of Glu (Fig. 3*E*). These results support the conclusion that in acinar cells secreted Glu is predominantly synthesized from Gln.

Glu is not accumulated in the ZGV. The secretion of free Glu occurs in unstimulated animals and was increased upon CCK stimulation as shown in Fig. 1*B*. To better understand the secretory mechanism of Glu, its possible accumulation in the ZGV was analyzed. Intact ZGVs (Fig. 4*A*) were used for Glu concentration analysis and the expression of Glu transporters in the ZGV membrane fraction. Glu, as well as Ala and Gln, was accumulated in the acinar cytosolic fraction and not in the ZGV (Fig. 4*B*). To enrich the ZGV membrane proteins, surface biotinylation of freshly purified ZGVs was performed before Glu transporter expression was analyzed by Western blot. Enrichment of the membrane fraction of the vesicles was indicated by the increase in the concentration of rab3D (specific ZGV membrane marker). With the use of MTSEA-biotin, the only Glu transporter detected in the ZGV membrane was the excitatory amino acid transporter EAAT1/GLAST-1 (Slc1a3) (Fig. 4*C*). Immunofluorescence staining suggests that EAAT1 was localized at the apical acinar cell membrane. The signal colocalized with the apical markers peanut agglutinin and actin-phalloidin. Although EAAT1 was immunoprecipitated with the ZGV membrane fraction, an intracellular EAAT1 signal was not observed in pancreatic tissue slices (Fig. 4*D*). These results could be explained by the presence of apical membrane material during the biotinylation or that the expression in ZGVs was too low to be detected by immunofluorescence. Taken together, these results support the conclusions that Glu was constitutively secreted and was not concentrated in ZGVs.

Glu is also accumulated in the pancreatic juice of animals fed a protein-deficient diet. Animals fed a protein -ree diet had reduced pancreatic mass and total protein content (Fig. 5, *A* and *B*). This adaptation was caused by the absence of protein arriving to the intestine, since sugar and fat were present and the diets were isocaloric, as described in METHODS. Additionally, animals showed an expected loss of body weight compared with animals maintained under control (20%) casein diet (Fig. 5, *C* and *D*). Despite decreased body weight and pancreatic volume, secreted pancreatic juice Glu concentrations were comparable to control animals fed the normal-protein diet. Pancreatic juice Glu was slightly but significantly elevated in animals fed the high-protein (40% casein) diet (Fig. 5*E*), but neither the protein-free nor high-protein diet condition resulted in significant changes relative to the control animals in plasma Glu concentrations (Fig. 5*F*). Therefore, pancreatic juice Glu levels were not regulated by the plasma concentration changes or passive transport.

We then analyzed the expression of Glu and Gln transporters and the accumulation of Gln in freshly isolated acinar cells from animals maintained in protein-free and high-protein diets. In acinar cells, isolated from animals maintained on a protein-free diet, SNAT5 (Slc38a5) expression was significantly decreased more than twofold at the RNA and protein levels (Fig. 6, *A* and *B*), whereas other transporters were not affected. However, neither the uptake of Gln (Fig. 6*C*) nor its oxidative metabolism was changed (Fig. 6*D*). Similarly, the oxidation of glucose and leucine was unchanged (Fig. 6*D*). We analyzed the expression of glutaminase (GLS), alanine and aspartate aminotransferases (GPT and GOT), asparagine synthetase (ASNS), and the branched chain aminotransferase (BCAT2), since we showed (Fig. 3) that the accumulation and secretion of Glu are dependent on Glu synthesis. Acinar cell GLS2 and GPT1 mRNA and protein levels were upregulated in animals maintained on a protein-free diet, while the protein expression of Glu dehydrogenase (Glud) was decreased (Fig. 6, *E* and *F*). BCAT2 and ASNS levels were unchanged and Glul expression was increased (Fig. 6*E*). Together, these results suggest that exocrine pancreas of rodents kept under protein restriction for short periods reduced protein synthesis, preserved Gln uptake and oxidative phosphorylation rate, and maintained free Glu secretion. We suggest that Glu accumulation was maintained by upregulation of enzymes synthesizing Glu from Gln.

Small intestine enterocyte proliferation is decreased in animals fed a protein-deficient diet. The mass of small intestine, crypts depth, and villi length were measured to provide an indirect measurement of the number of cells and cellular proliferation. For animals fed a protein-deficient diet, the intestinal mass of jejunum and ileum was only slightly and nonsignificantly reduced (Fig. 7*A*). Analysis of villi length indicated a reduction in cell number in the jejunum (Fig. 7*B*). Villi shortening can be caused by a reduction in crypt cell proliferation, an increase in cell cycle length, the differentiation and migration of the cells toward the tip of the villi, or an increase of anoikis (56, 73). In the animals receiving the protein-deficient diet, the depth of crypts was decreased in jejunum and ileum (Fig. 7*C*), but the proliferation marker Ki67 was reduced only in the jejunum (Fig. 7*D*) coinciding with a decrease in villi length. In addition, the expression of cyclins involved in the G_1/S checkpoint (cyclin E2 and D1) was also

Fig. 3. Acinar cells metabolize glutamine (Gln) to generate energy and to synthesize glutamate (Glu). *A*: acinar cells preferentially metabolize Gln as source of energy. Metabolization of ^{14}C-labeled substrate was measured in freshly isolated mouse acinar cells by the CO_2-trapping method. The results are expressed as nmol·h^{-1}·μg DNA^{-1} and reported as means ± SE; $n = 3$ mice. *B*: acinar cells and AR42J cells express the enzymes involved in Glu metabolism. Enzymes mRNA expression in isolated rat acinar cells (black bars) and AR42J cells (hatched bars) was measured by quantitative (q)PCR. Values are expressed relative to 18S RNA. Glul, glutamine synthase; Glud, glutamate dehydrogenase; gls1 and 2, glutaminase 1 and 2; got1 and 2, aspartate aminotransferase 1 and 2; gpt1 and 2, alanine aminotransferase 1 and 2. *C*: inhibition of glutaminase decreased Glu accumulation in AR42J cells. Amino acid concentration was measured by UPLC in AR42J cells treated with the glutaminase inhibitor 6-diazo-5-oxo-L-norleucine (DON; 250 μM), the alanine aminotransferase inhibitor L-cycloserine (CySer; 250 μM), or the aspartate aminotransferase inhibitor aminooxy-acetic acid hemihydrochloride (AOA; 250 μM). Results (means ± SE) are expressed as nmol/μg DNA; $n = 3$–6 wells. $^*P < 0.05$, $^{***}P < 0.001$ (two-way ANOVA with post hoc Bonferroni test). *D*: DON does not inhibit Gln transport. Uptake of Gln (1 mM), Glu (1 mM), or glucose (25 mM) was measured in AR42J cells treated with DON (black bars) and in untreated cells (white bars). The results (means ± SE) are expressed as nmol·2 min^{-1}·μg DNA^{-1}; $n = 9$–15 wells per treatment. *E*: freshly isolated mouse acini accumulated and secreted Glu when incubated with Gln. Glu concentration was measured with Amplex system in the medium and acini incubated in the presence of BSA (control) or 2 mM Gln, Ala, or Leu. Glutaminase was inhibited with DON (250 μM) (gray bars). Results (means ± SE) are expressed as nmol/μg DNA and normalized to the control group; $n = 6$ mice, $^*P < 0.05$, $^{**}P < 0.01$, $^{***}P < 0.001$ (ANOVA with post hoc Bonferroni test).

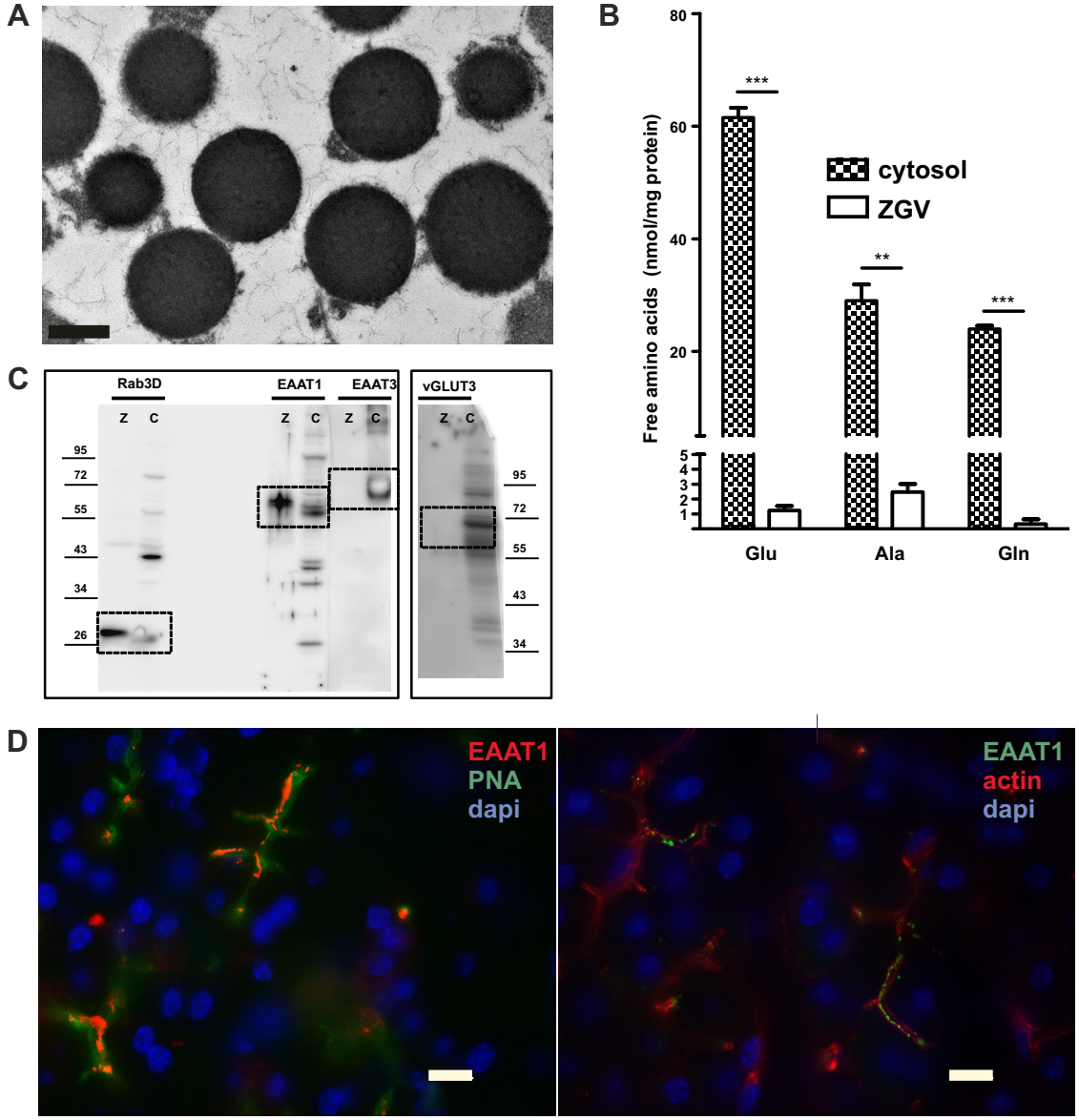

Fig. 4. Glutamate (Glu) is not concentrated in the zymogen granules vesicles (ZGVs). *A*: electron microscopy revealed intact mouse ZGVs. The images of fixed preparation were performed with transmission electron microscope Philips CM100 (1994, 40–100 kV), equipped with digital camera. Magnification: ×17,500; bar length: 0.5 μm. *B*: Glu is not accumulated in ZGVs. Cytosolic (hatched bars) and ZGV (white bars) fraction amino acid concentration was measured by UPLC. Amino acid concentration was normalized to the protein content. The results are given as means ± SE; $n = 4$ mice. $^{**}P < 0.01$, $^{***}P < 0.001$ (ANOVA with post hoc Bonferroni test). *C*: the amino acid transporter EAAT1 is expressed at the ZGV membrane. Representative Western blot of surface biotinylated zymogen granules vesicle membranes (Z) and total membrane of control organs (C, control; for rab3D; pancreas; for EAAT1, brain; for EAAT3, kidney; and for vGLUT3, crude brain synaptosomes). Noncontiguous stripes containing the surface biotinylated ZGVs and tissue control are showed lined. Rab3D, EAAT1, and EAAT3 were electrophoresed in the same 10% agarose gel and vGLUT3 in a 8% gel. *D*: the Glu transporter EAAT1 is localized apically in acinar cells. *Left*: a mouse pancreas cryosections (9 μm) stained for EAAT1 (red) and for the apical acinar cell marker peanut agglutinin (PNA; green). *Right*: EAAT1 (green) is shown to colocalize with actin-Phalloidin (red). Nuclei are stained in blue (DAPI). Magnification: ×100; bar length: 10 μm.

decreased in the jejunum of animals fed a protein-deficient diet (Fig. 7*E*). The rate of detachment induced apoptosis (anoikis) was verified by caspase 3 expression, which was lower in animals receiving the protein depleted diets (Fig. 7*F*). These observations suggest that in the animals receiving a protein-deficient diet the renewal rate of jejunal villi was reduced. The loss of epithelial barrier tightness is another alteration that can follow malnourishment. The mRNA and protein levels of the tight junction proteins occludin and ZO-1 were analyzed along the length of the small intestine (Fig. 7, *F* and *G*). We observed no changes on the mRNA level. At the protein level, ZO-1 expression was increased slightly in the ileum and occludin was unchanged. The mucus layer integrity was indirectly analyzed by the expression of secreted mucin (mucin 2). The expression of mucin 2 mRNA was higher toward the ileum and did not differ in the groups receiving different diets. This data agrees with the periodic acid-Schiff staining of the rat samples showing normal number and distribution of goblet cells (data not shown). Together these data suggest that there was no loss of barrier function.

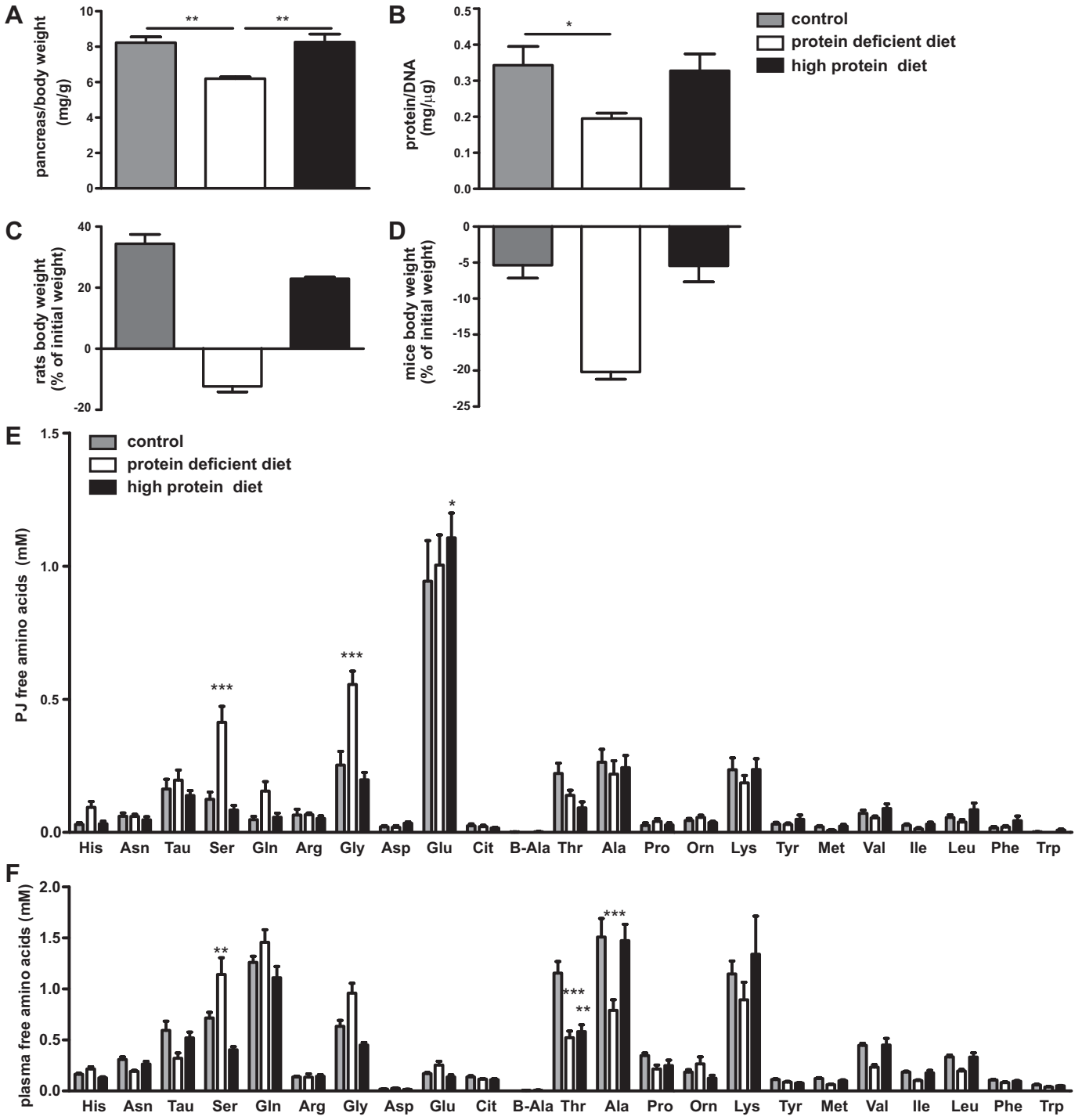

Fig. 5. Protein-deficient diet induced a decrease in pancreas volume and total protein but had no effect on glutamate (Glu) secretion in the pancreatic juice. *A* and *B*: volume (*A*) and total protein (*B*) in pancreas. Mice were kept on protein-deficient (white bars), control (gray bars), and high-protein (black bars) diet. *A*: at the end of the treatment, body and pancreas weights were measured and the ratio plotted (mg/g). *B*: freshly isolated acini were prepared from these animals and the total protein and DNA content were measured (μg/mg). The results are given as means ± SE; $n = 3$–9 mice. *$P < 0.05$, **$P < 0.01$ (ANOVA with post hoc Bonferroni test). *C* and *D*: body weight in rats (*C*) and mice (*D*). Body weight of rats (*C*) and mice (*D*) were measured after treatment with protein-deficient (white bars), control (gray bars), and high-protein (black bars) diet. The results are expressed as percentage of the initial weight and are given as means ± SE; $n = 6$–9 mice and 7 rats per diet. *E*: amino acid concentration in pancreatic juice. Amino acid concentration was analyzed by UPLC in pancreatic juice of rats were fed protein-deficient (white bars), control (gray bars), and high-protein (black bars) diet. Results are given as means ± SE; $n = 7$ rats per diet. *$P < 0.05$, ***$P < 0.001$ (two-way ANOVA with post hoc Bonferroni test). *F*: plasma amino acid concentration. After collection of pancreatic juice, heart blood was sampled and the plasma amino acid concentration analyzed by UPLC. Results are given as means ± SE; $n = 7$ rats per diet. **$P < 0.01$, ***$P < 0.001$ (two-way ANOVA with post hoc Bonferroni test).

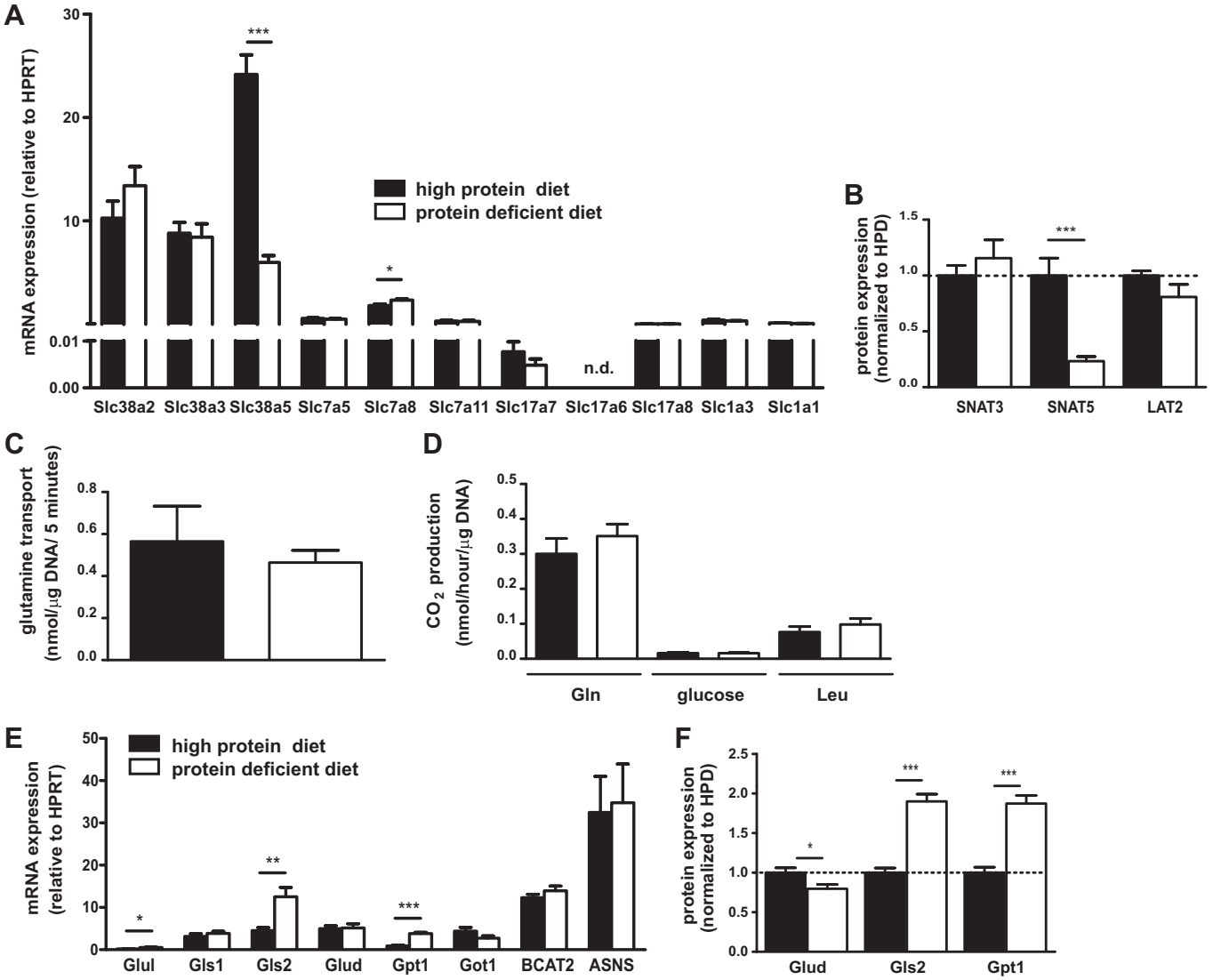

Fig. 6. Protein-deficient diet did not affect glutamine (Gln) transporters expression and uptake but induced increase in glutaminase and alanine aminotransferase expression. *A* and *B*: expression of amino acid transporters. *A*: pancreas of mice fed high-protein (black bars) and protein-deficient (white bars) diet was used to analyze the expression of amino acid transporters by qPCR. Transporters mRNAs analyzed were Slc38a2/SNAT2, Slc38a3/SNAT3, Slc38a5/SNAT5, Slc7a5/LAT1, Slc7a8/LAT2, Slc7a11/xCT, Slc17a7/vGLUT1, Slc17a6/vGLUT2, Slc17a8/vGLUT3, Slc1a1/EAAT3, and Slc1a3/EAAT1. Results are expressed relative to hypoxanthine phosphoribosyltransferase (HPRT) mRNA and given as means ± SE; $n = 6$ mice per diet. $^{*}P < 0.05$, $^{***}P < 0.001$ (multiple two-tailed *t*-tests). *B*: the expression of transporters SNAT3, SNAT5, and LAT2 was also tested at protein level by Western blot. The relative expression to actin was normalized to high-protein diet (HPD, black bars). The results are given as means ± SE; $n = 6$ mice per diet. $^{***}P < 0.001$ (multiple two-tailed *t*-tests). *C* and *D*: Gln transport and Gln oxidation in acini. *C*: freshly isolated acini prepared from mice under high-protein (black bars) and protein-deficient (white bars) diet were incubated with Gln (1 mM) for 5 min. The results are normalized to DNA content and are given as means ± SE; $n = 6$–9 per diet. *D*: the ^{14}C-labeled substrate metabolization was measure in freshly isolated mouse acinar cells by the CO_2-trapping method in acini prepared from mice under high-protein (black bars) and protein-deficient (white bars) diet. The results are given as means ± SE; $n = 6$–9 mice per diet. *E* and *F*: enzymes involved in Glu synthesis. *E*: enzyme expression was analyzed in pancreas of mice fed high-protein (black bars) and protein-deficient (white bars) diet by qPCR. Glul, Gln synthase; gls1 and 2, glutaminase 1 and 2; Glud, glutamate dehydrogenase; gpt1 and 2, alanine aminotransferase 1 and 2; got1 and 2, aspartate aminotransferase 1 and 2. Results are expressed relative to the HPRT mRNA and given as means ± SE; $n = 6$ mice per diet. $^{*}P < 0.05$, $^{**}P < 0.01$, $^{***}P < 0.001$ (multiple two-tailed *t*-tests). *F*: the expression of glutamate dehydrogenase (Glud), glutaminase (Gls2), and alanine aminotransferase (Gpt1) was analyzed at protein level by Western blot. Protein expression relative to actin was normalized to high-protein diet (HPD, black bars). The values are given as means ± SE; $n = 6$ mice per diet. $^{*}P < 0.05$, $^{***}P < 0.001$ (multiple two-tailed *t*-tests).

The metabolism but not the transport of Glu is altered in the small intestine during protein restriction. The Glu arriving into the lumen of the small intestine is transported into the enterocytes where it is metabolized for energy production or exported to the body. The Glu transporter EAAT3/EAAC1, a member of the excitatory amino acid family (Slc1a1), is the only transporter identified in enterocytes for dicarboxylic amino acids (36). This high affinity Na^+-dependent transporter is localized at the apical membrane of the enterocyte, toward the crypts as depicted in Fig. 8*A*. EAAT3 does not colocalize with B^0AT1, a neutral amino acids transporter localized at the tip of the villi. Uptake experiments with two concentrations of Glu [10 μM (Fig. 8*B*) and 1 mM (Fig. 8*C*)] in the presence and absence of Na^+ were performed. Only slight nonsignificant diet-induced

changes were observed. High-affinity Na^+-dependent transport of Glu, likely reflecting EAAT3 activity, tended to be reduced in the jejunum under a protein-free diet whereas the unknown low-affinity Na^+-dependent transport of Glu was slightly increased in the ileum. As a control, the Na^+-dependent transport of Leu, attributed to B^0AT1, was analyzed and also found to be unchanged (Fig. 8*D*). Interestingly, the RNA and protein expression of B^0AT1 were reduced in the jejunum of animals fed the protein-free diet, while that of EAAT3 was increased (Fig. 8*E*). Even though we did not observe changes in transport

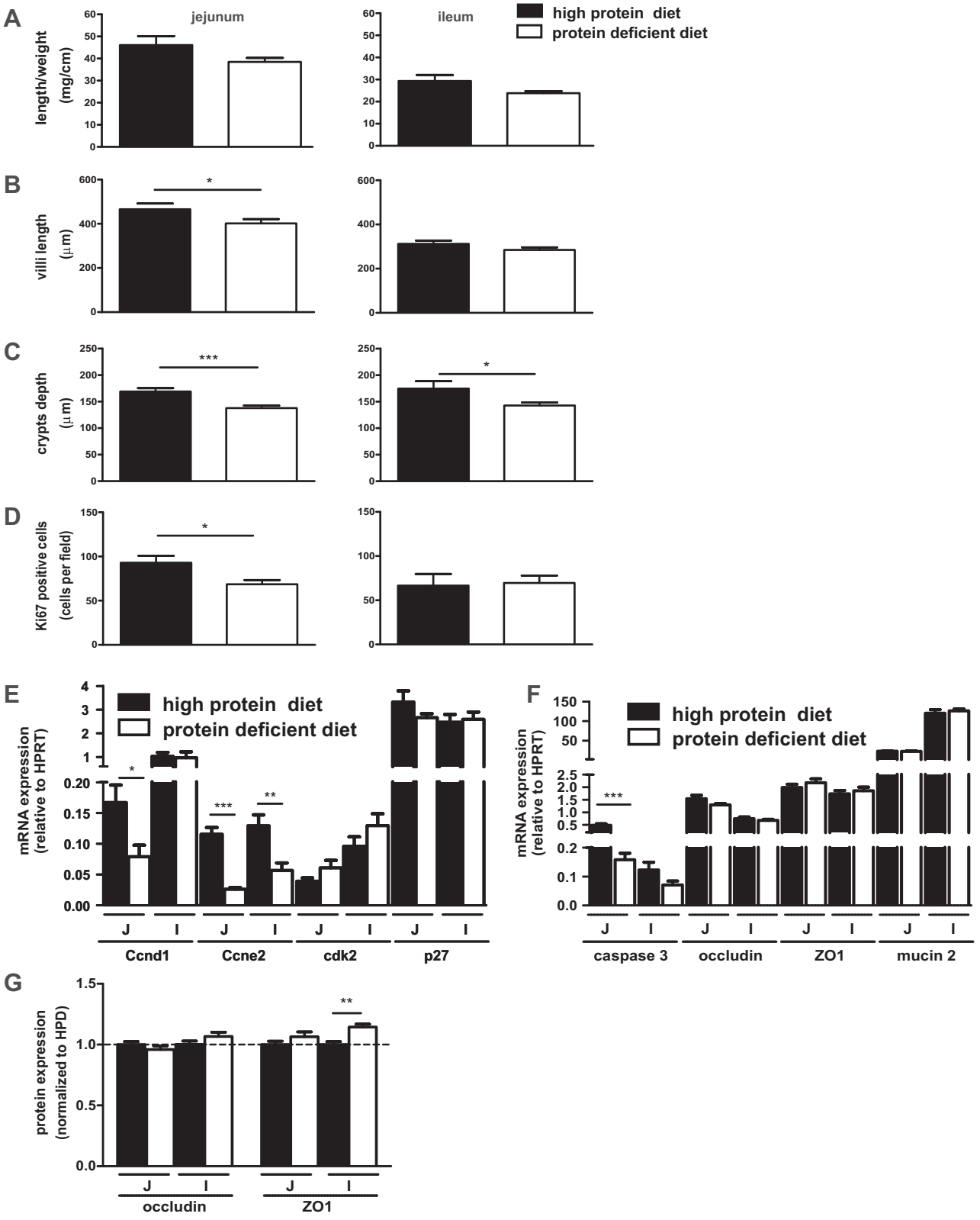

capacity of Glu, the expression of enzymes involved in Glu metabolism was changed in enterocytes. As depicted in Fig. 9*A*, Glud protein expression was increased in enterocytes of animals fed a protein-deficient diet. The aminotransferases (GOT and GPT) expression at mRNA level had a tendency to decrease and Gln synthase increased in these animals (Fig. 9*B*). The changes in Glud expression suggest that although cells did not accumulate increased amounts of Glu, they more efficiently metabolized Glu to produce energy. Together these data suggest that during protein diet restriction, metabolism of Glu secreted from the acinar cells to the small intestine lumen was altered to maintain enterocyte energy production.

DISCUSSION

Our findings suggest that one mechanism by which Gln exerts a positive effect on exocrine pancreas and small intestine involves its uptake and metabolism to Glu in acinar cells and secretion into the lumen of the small intestine. Importantly, under protein restriction, pancreatic secretion of Glu into the lumen of the small intestine was maintained. Pancreas and small intestine transport capacity for Gln or Glu, respectively, was not altered, but the expression of enzymes involved in the synthesis of Glu in the pancreas and in the metabolism of Glu in the small intestine was increased. These data suggest an adaptation to the more efficient use of Gln and Glu by acinar cells and enterocytes. This complementary interorgan use of Gln-Glu may become especially important under nutrient shortage. However, longer periods of protein restriction and starvation, which may activate different and or additional survival mechanisms, were not analyzed in this study.

Secretion of free amino acids by the exocrine pancreas. The presence of free amino acids in the secretion of exocrine glands, such as the salivary, lacrimal, and mammary glands, has been previously reported, but their role is not always clear (53, 66). In maternal milk, Glu concentration is higher than that of any other amino acid and almost tenfold higher than in plasma. Additionally, the amino acids Gln, alanine, and aspartate are also highly concentrated in milk (58). In pancreatic juice, Glu and aspartate, but not neutral amino acids, were more concentrated. Pancreatic Glu secretion occurred during basal and increased under cholecystokinin induction (CCK-8 peptide), suggesting ZGVs could be involved in the accumulation and release of Glu, as proposed for β-cells (28, 43, 49). In β-cells, the vesicular transporter (vGLUT3/Slc17a8) and EAAT2/Slc1a2 were suggested to accumulate Glu and regulate pH in the vesicles (26). However, EAAT2 expression is very low and its ablation did not change Glu accumulation and release (74). As for islets, we also detected a member of the sodium-dependent excitatory amino acid family (EAAT1/GLAST1/Slc1a3) in the ZGV membrane. However, by immunofluorescence we could not confirm its localization to the zymogen granules; rather it was localized in the apical membrane. Since the transport stoichiometry and mechanism do not support a role in Glu efflux, the physiological role of EAAT1 in acinar cells remains unclear. As previously shown for other solutes (30), Glu secretion may take place via active transport on the apical plasma membrane. Therefore, a still unknown carrier, active during basal and stimulated secretion, may be responsible for the secretion of Glu by pancreatic acinar cells.

Origin of Glu secreted by the exocrine pancreas. We found that the exocrine pancreatic secretion is rich in Glu consistently with previous reports by Fukushima et al. (25) and that it originates from the metabolism of neutral amino acids. Similarly to exocrine pancreas, it has been show by others that the lactating mammary cells secreted Glu is synthesize from neutral amino acids. Mammary cells indeed avidly take up Leu that is metabolized to Glu by the branched chain amino acid aminotransferase (BCAT) (49). In contrast, we show here that in pancreatic acinar cells, although BCAT is expressed, Leu did not stimulate Glu secretion. Schachter and Buteau (57) also demonstrated that in pancreatic slices the Glu produced from Leu was accumulated intracellularly and that the secreted Glu originates mostly from Gln. We additionally show here that Leu was not an efficient source of energy for acinar cells that preferred to utilize Gln in comparison to Leu, glucose, or palmitoyl. Consistent with this observation, intravenously administered Gln was shown to accumulate rapidly in pancreas (14, 51). Furthermore, we demonstrated here that acinar cells express both enzymes (Gls and Glud) required for Glu synthesis from Gln and for further channeling into the TCA cycle. In addition, the inhibition of glutaminase efficiently decreases Glu secretion. Thus Glu accumulation in the lactating mammary gland and in acinar cells results from intracellular synthesis and not from active transport of the excitatory amino acid. That acinar cells use a more abundant substrate for the synthesis of Glu is compatible with the composition and period of the secretion. In contrast to milk, pancreatic juice is produced constitutively throughout life and does not accumulate neutral amino acids or Gln. The fact that both milk and pancreatic juice ultimately reach the lumen of the small intestine highlights the potentially important role of Glu for enterocytes and leads us to propose that Glu is utilized in energy transfer.

Fig. 7. Small intestine enterocyte proliferation is decreased in animals fed a protein-deficient diet. *A*: volume of jejunum and ileum. The small intestine segments were weighed and measured. The values are expressed as mg/cm and given as means ± SE; $n = 3$–5 mice per diet. *B*: villi length. The fixed rat small intestine segments were stained with hematoxylin-eosin. The length of the villi was analyzed in ×4 magnification pictures. Results are expressed in μm and given as means ± SE; $n = 9$–18 villi from 2 to 3 rats per segment per diet. $^*P < 0.05$ (multiple two-tailed *t*-tests). *C*: crypts depth. The crypts depth was analyzed in ×40 magnification pictures. Results are expressed in μm and given as means ± SE; $n = 6$–27 crypts from 2 to 3 rats per segment per diet. $^*P < 0.05$, $^{***}P < 0.001$ (multiple two-tailed *t*-tests). *D*: Ki67 quantification. The number of positive Ki67 cells was analyzed in ×40 magnification pictures. Results are expressed in positive Ki67/field and given as means ± SE; $n = 10$–16 fields from 2 to 3 rats per segment per diet. $^*P < 0.05$ (multiple two-tailed *t*-tests). *E*: expression of cell cycle components. Small intestine of mice was used for mRNA expression analysis of ccnd1, ccne2, cdk2, and p27 (or kip/cdkn1b) by qPCR. *F*: caspase 3 and tight junction protein and mucin 2 mRNA expression. Small intestine was used for the expression of caspases 3, occludin, zonula occludens-1 (ZO-1), and mucin2 by qPCR. Results are expressed relative to HPRT and given as means ± SE; $n = 6$ mice per diet. $^*P < 0.05$, $^{**}P < 0.01$, $^{***}P < 0.001$ (multiple two-tailed *t*-tests). *G*: tight junction protein expression. The expression of ZO-1 and occludin protein was analyzed by Western blot. The results are expressed relative to NaKATPase and normalized to high-protein diet (HPD). Data are means ± SE; $n = 6$ mice per diet. $^{**}P < 0.01$ (multiple two-tailed *t*-tests). Black bars: mice fed high-protein diet; white bars: mice fed protein-deficient diets.

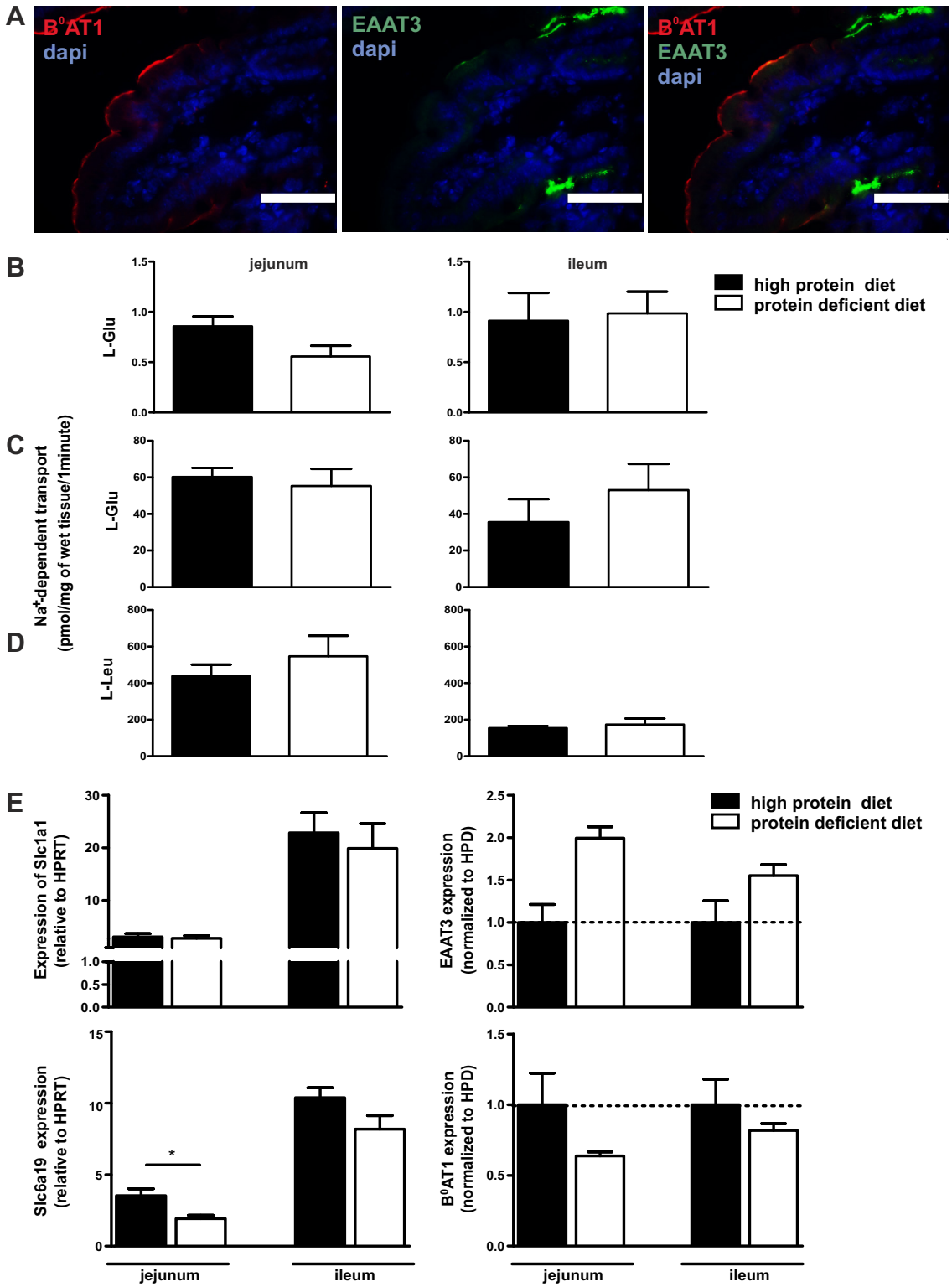

Fig. 8. Amino acid transporters expression levels do not reflect the transport capacity of amino acids in small intestine. *A*: EAAT3 and B0AT1 localization. Paraffin-embedded mouse intestine was stained for EAAT3/EAAC1 (green) and B^0AT1 (red) and nuclei are stained in blue (DAPI). *Left*: depicts only B^0AT1 (red). *Middle*: depicts only EAAT3/EAAC1 (green). *Right*: depicts both transporters. Magnification: ×60; bar length: 50 μm. *B* and *C*: Na^+-dependent transport of glutamate (Glu). Everted rings from jejunum (*left*) and ileum (*right*) were incubated with 10 μM (*B*) or 1 mM (*C*) Glu. Results are expressed as sodium-dependent transport in pmol·mg wet $tissue^{-1}$·1 min^{-1} and given as means ± SE; n = 6–9 mice per group. *D*: Na^+-dependent transport of leucine. Everted rings were incubated with 1 mM leucine. Results are expressed as sodium-dependent transport in pmol·mg wet $tissue^{-1}$·1 min^{-1} and given as means ± SE; n = 3–5 mice per group. *E*: expression of EAAT3 and B0AT1. The mRNA expression (*left*) of EAAT3 (slc1a1) and B^0AT1 (slc6a19) was analyzed by qPCR and is expressed relative to HPRT mRNA. The expression of EAAT3 and B^0AT1 protein (*right*) was analyzed by Western blot. The results are expressed relative to NaKATPase and normalized to high-protein diet (HPD). Data are means ± SE; n = 6 mice per diet. *$P < 0.05$ (multiple two-tailed t-tests). Black bars: mice fed high-protein diet; white bars: mice fed protein-deficient diets.

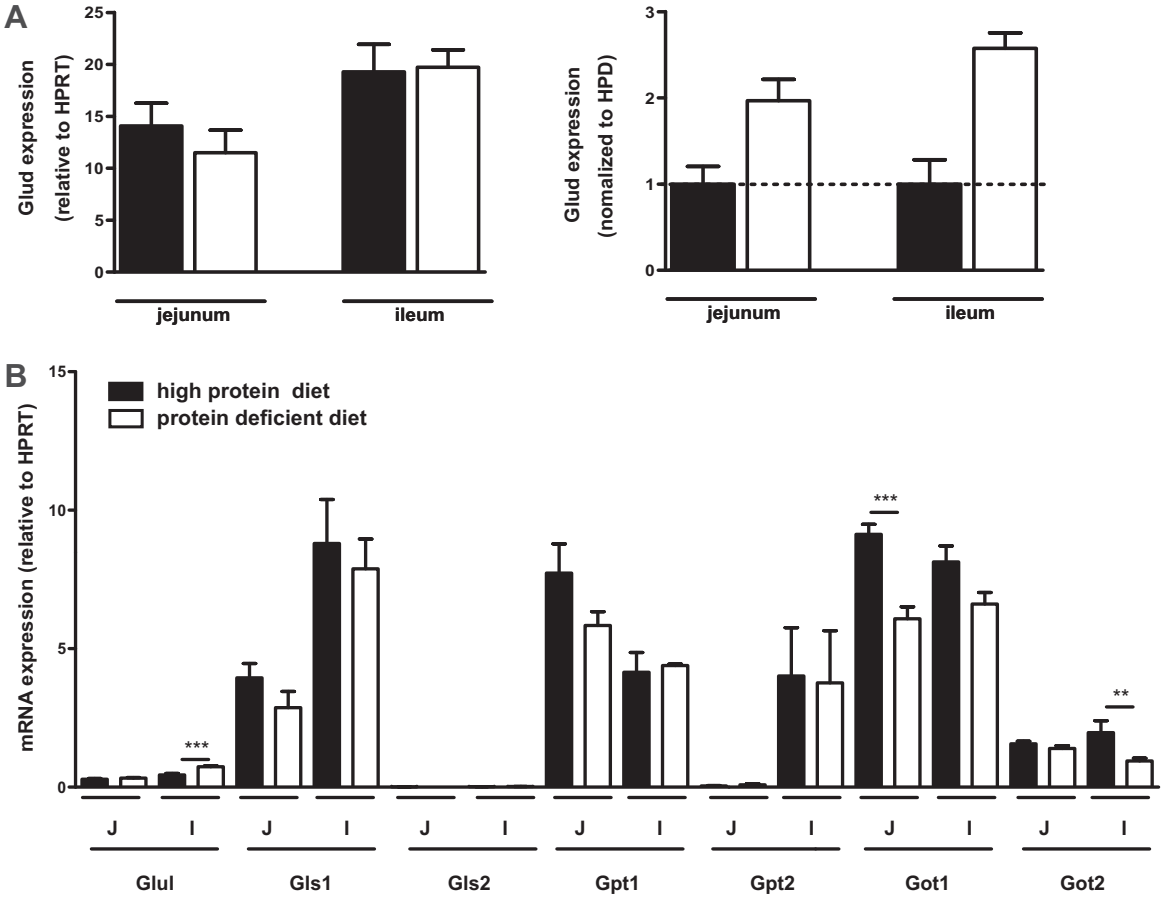

Fig. 9. Glutamate dehydrogenase (Glud) expression is increased in animals under a protein-restriction diet. *A*: Glud expression. The expression of Glud was analyzed at RNA (*left*) and protein level (*right*). The expression of Glud in mice fed high-protein diet (black bars) and protein deficient (white bars) were analyzed by quantitative qPCR (*left*) and Western blot (*right*). Glud mRNA is expressed relative to HPRT mRNA. Protein is expressed relative to NaKATPase and normalized to high-protein diet (HPD, black bars). Results are means ± SE; $n = 6$ mice per diet. *B*: small intestine expression of enzymes involved in Glu metabolism. Small intestine of mice fed high-protein (black bars) and protein-deficient (white bars) diets was used for mRNA expression by qPCR. Results are expressed relative to the HPRT and given as means ± SE; $n = 6$ mice per diet. $^{**}P < 0.01$, $^{***}P < 0.001$ (multiple two-tailed *t*-tests). Glul, glutamine synthase; gls1 and 2, glutaminase 1 and 2; gpt1 and 2, alanine aminotransferase 1 and 2; got1 and 2, aspartate aminotransferase 1 and 2.

Maintaining Glu secretion during protein restriction. During total parenteral nutrition and protein-deficient diet, the exocrine pancreatic volume and the synthesis of digestive enzymes are diminished (3, 18). However, despite the reduction of pancreas volume and protein synthesis, the secretion of free Glu was unchanged in our animals receiving a protein-deficient diet. The fact that Glu secreted by acinar cells mainly results from imported Gln suggested that maintaining the expression of neutral amino acid transporters may be important to sustaining Glu secretion during malnutrition. We report here that an acute depletion of dietary proteins did not influence neutral amino acid transporters expression in acinar cells, with the exception of a strong decrease of SNAT5/Slc38a5. SNAT5 reduced expression did not impact on Gln uptake. This lack of effect may be explained by its transport mode and the presence of other transporters. It has been demonstrated in astrocytes that SNAT5 favors Gln efflux rather than influx (75). Additionally, Gln can be accumulated in acinar cells by the other transporters displaying various kinetic modes [symporters and antiporters (exchangers), sodium dependent and independent] and affinities (μm to mM range). The mechanism by which SNAT5 expression is regulated during protein restriction and its effect on acinar cells are unknown. In highly proliferating cells, SNAT5 was shown to be directly targeted by cMyc, increasing its expression (67). Other members of the SNATs (Slc38) family were suggested to play a role in signaling under starvation and cell volume changes via the m mammalian target of rapamycin pathway (15, 47, 54). It was also recently shown that depletion of two substrates of SNAT5, Gln and serine, activates the tumor suppressor p53 (10, 40). p53 Induced by amino acid depletion increases the expression of prosurvival genes, for example, Gls2 (9, 53), which was also increased in pancreas of animals maintained on a protein-deficient diet. The increase in Gls2 expression and activity is suggested to support cell survival by increasing NADH production, ameliorating the redox balance of the cells and providing protection from reactive oxygen species. Additionally, Glu participates in glutathione synthesis and feeds the TCA cycle (34, 68, 69). Gls2 increased expression could also explain the maintenance of Glu synthesis and secretion under protein restriction. Whether there is a connection between SNAT5 downregulation and the prosurvival mechanism activation of Gls2 expression in acinar cells during protein restriction is not known. Based on our results, we suggest that acinar

cells adapt to protein depletion and amino acid availability via metabolic regulation rather than via increasing amino acid transporter expression.

Fate of Glu in the small intestine. We found that Glu transport was maintained and the expression of the enzyme Glud increased in enterocytes of animals fed protein-deficient diet. Luminal Glu is the most efficiently metabolized substrate in enterocytes, although arterial glucose and Gln also play roles in providing energy to intestinal epithelial cells (12, 46, 52). Boutry et al. (6) suggested that the high enterocyte metabolism of luminal Glu, rather than luminal or arterial Gln, spare Gln as a metabolic fuel. In this context, the release of Glu from

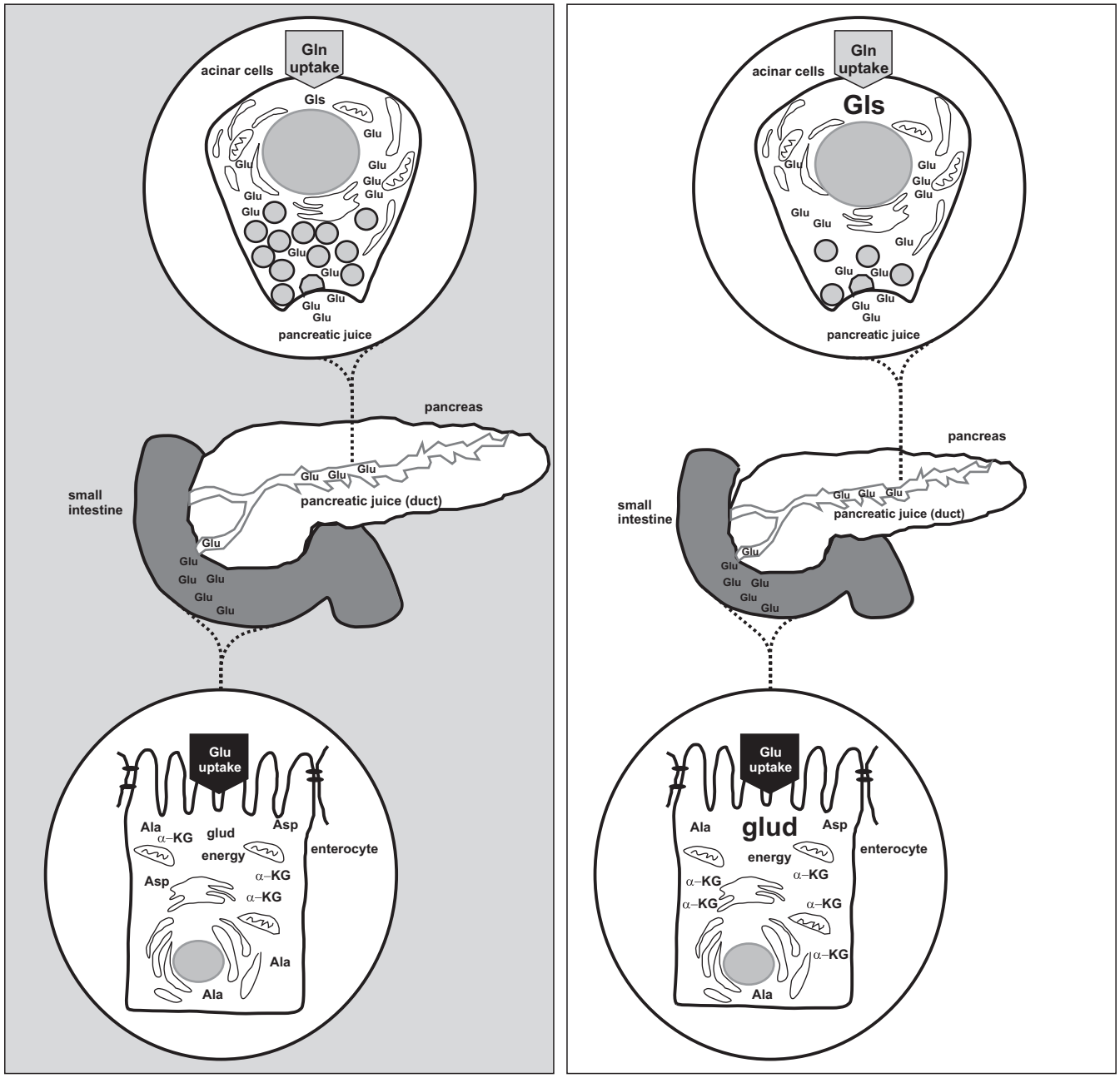

Fig. 10. Schematic representation of how pancreatic juice glutamate (Glu) secretion sustains enterocytes nutritional needs under short period of protein-deficient diet consumption. Under protein restriction (*right*, white field), the protein content and the volume of the pancreas is reduced compared with normal or high-protein diet (*left*, gray). The transport of glutamine (Gln uptake, gray arrowhead) into acinar cells of the exocrine pancreas of animals fed protein-deficient diet is not different to animals receiving high-protein diet. Once into the acinar cells, Gln is metabolized by glutaminase (Gls) toward Glu. The Gls expression is upregulated in acinar cells under a protein-restriction diet and the Glu secretion in the pancreatic juice (PJ) is similar to the animals receiving normal- or high-protein diet. We suggest that the level of Glu secretion in the PJ is maintained by the Gls upregulation. The secreted Glu in the PJ reach the lumen of the small intestine and is efficiently absorbed by the enterocytes (Glu uptake, black arrowhead). In the enterocytes of animals under protein restriction, Glu transport capacity was not altered. Once in the cells, Glu is metabolized by the enzyme glutamate dehydrogenase (Glud) to generate α-ketoglutarate (α-KG). The expression of Glud in the enterocytes of animals under protein restriction is augmented, allowing these cells to more efficiently metabolize Glu to α-KG. α-KG can feed the Krebs cycle and maintain energy production. The preservation of Gln transport in acinar cells and Glu in the enterocytes additionally with the metabolic adaptation in these cells may play an important role to sustain pancreatic and intestinal homeostasis under protein-deprivation periods.

pancreatic juice may be important for maintaining intestinal homeostasis under protein starvation. The site of the highest Glu metabolism may be the villi, where enzymes involved in the metabolism of Glu are localized (72). The only transporter for Glu identified in small intestine enterocytes is the high-affinity sodium-dependent transporter EAAT3 (Slc1a1), which is however localized toward the crypts (22, 36). Therefore, Glu absorption may involve other unknown carrier(s) as was recently proposed by Fanjul et al. (23). That the absorption of Glu and Leu were unchanged in our animals challenged with protein-deficient diet may be due to the high transport capacity of small intestine enterocytes. The absorptive capacity of Glu in the intestine was estimated to be fourfold higher than the normal amount ingested daily (37). For that reason, minor changes in transporters may not cause significant changes in total or in sodium-dependent transport. Although absorptive capacity was not changed, a reduction in proliferation and the continuous renewal of the epithelia were observed, suggesting that cells changed from a highly proliferating to a more quiescent state under protein restriction. The physiological transition from proliferating to quiescent cells involves metabolic adaptations, and Glu is central for these adaptations. In quiescent epithelial cells, Glud expression is increased and Glu metabolism is driven toward the production of energy. In the proliferative phase, aminotransferases metabolism of Glu is favored additionally generating nonessential amino acids to support protein synthesis (16). In our animals receiving a protein-deficient diet, the increase in Glud expression and reduced cell proliferation suggests that enterocytes adapted their metabolism to the temporary nutrient deprivation. As we also observed in acinar cells, enterocyte adaptations under protein restriction altered metabolism rather than amino acids transport into cells. The possible advantage of this strategy may be to quickly accumulate substrates as soon as available without the energy costs of transcribing and translating new transporters.

In summary and as depicted in Fig. 10, we suggest an interorgan relationship between exocrine pancreas and small intestine for Gln-Glu utilization. This involves the uptake and metabolism of Gln in acinar cells, the secretion of Glu into the lumen of the small intestine and the uptake and use of Glu by enterocytes. As recently showed by Colloff et al. (16), epithelial cells may modulate their Gln-Glu metabolism to cope with physiological needs. Likewise, our results suggested that under protein restriction the exocrine pancreas Glu secretion is maintained by upregulation of Glu-synthesizing enzymes and in the enterocytes Glu utilization by upregulation of Glu-metabolizing enzyme without changes in transport capacity of amino acids. Additional studies are necessary to identify the secretory mechanism of Glu and further characterize the up- and downstream mechanisms controlling the metabolic adaptation in acinar cells.

ACKNOWLEDGMENTS

We thank Birgit Roth Z'graggen and Peter Hunziker for assistance and support for the amino acid measurements at the Functional Genomics Center Zurich. We also thank Victoria Makrides and Ian C. Forster (Institute of Physiology, University of Zurich and Florey Institute of Neuroscience and Mental Health, Melbourne, Australia) for valuable suggestions for the manuscript.

GRANTS

This work was financially supported by University of Zurich and Swiss National Science Foundation.

DISCLOSURES

No conflicts of interest, financial or otherwise, are declared by the authors.

AUTHOR CONTRIBUTIONS

S.A., E.K., and S.M.C. conceived and designed research; S.A., D.G., L.M., C.L., and S.M.C. performed experiments; S.A., D.G., C.L., and S.M.C. analyzed data; S.A., E.K., D.G., T.V.R., R.G., F.V., and S.M.C. interpreted results of experiments; S.A., D.G., and S.M.C. prepared figures; S.A., E.K., D.G., C.L., and S.M.C. drafted manuscript; S.A., E.K., L.M., T.V.R., R.G., F.V., and S.M.C. edited and revised manuscript; S.A., E.K., D.G., L.M., C.L., T.V.R., R.G., F.V., and S.M.C. approved final version of manuscript.

REFERENCES

1. **Altman BJ, Stine ZE, Dang CV.** From Krebs to clinic: glutamine metabolism to cancer therapy. *Nat Rev Cancer* 16: 619–634, 2016.[Erratum. *Nat Rev Cancer* 16: 773, 2016.] doi:10.1038/nrc.2016.71.
2. **Asrani V, Chang WK, Dong Z, Hardy G, Windsor JA, Petrov MS.** Glutamine supplementation in acute pancreatitis: a meta-analysis of randomized controlled trials. *Pancreatology* 13: 468–474, 2013. doi:10.1016/j.pan.2013.07.282.
3. **Baumler MD, Koopmann MC, Thomas DD, Ney DM, Groblewski GE.** Intravenous or luminal amino acids are insufficient to maintain pancreatic growth and digestive enzyme expression in the absence of intact dietary protein. *Am J Physiol Gastrointest Liver Physiol* 299: G338–G347, 2010. doi:10.1152/ajpgi.00165.2010.
4. **Beaulieu AD, Drackley JK, Overton TR, Emmert LS.** Isolated canine and murine intestinal cells exhibit a different pattern of fuel utilization for oxidative metabolism. *J Anim Sci* 80: 1223–1232, 2002. doi:10.2527/2002.8051223x.
5. **Boelens PG, Nijveldt RJ, Houdijk AP, Meijer S, van Leeuwen PA.** Glutamine alimentation in catabolic state. *J Nutr* 131, *Suppl*: 2569S–2577S, 2001. doi:10.1093/jn/131.9.2569S.
6. **Boutry C, Bos C, Matsumoto H, Even P, Azzout-Marniche D, Tome D, Blachier F.** Effects of monosodium glutamate supplementation on glutamine metabolism in adult rats. *Front Biosci (Elite Ed)* 3: 279–290, 2011.
7. **Brannon PM.** Adaptation of the exocrine pancreas to diet. *Annu Rev Nutr* 10: 85–105, 1990. doi:10.1146/annurev.nu.10.070190.000505.
8. **Bröer A, Rahimi F, Bröer S.** Deletion of amino acid transporter ASCT2 (SLC1A5) reveals an essential role for transporters SNAT1 (SLC38A1) and SNAT2 (SLC38A2) to sustain glutaminolysis in cancer cells. *J Biol Chem* 291: 13194–13205, 2016. doi:10.1074/jbc.M115.700534.
9. **Budanov AV.** The role of tumor suppressor p53 in the antioxidant defense and metabolism. *Subcell Biochem* 85: 337–358, 2014. doi:10.1007/978-94-017-9211-0_18.
10. **Budanov AV.** Stress-responsive sestrins link p53 with redox regulation and mammalian target of rapamycin signaling. *Antioxid Redox Signal* 15: 1679–1690, 2011. doi:10.1089/ars.2010.3530.
11. **Bürki R, Mohebbi N, Bettoni C, Wang X, Serra AL, Wagner CA.** Impaired expression of key molecules of ammoniagenesis underlies renal acidosis in a rat model of chronic kidney disease. *Nephrol Dial Transplant* 30: 770–781, 2015. doi:10.1093/ndt/gfu384.
12. **Burrin DG, Stoll B.** Metabolic fate and function of dietary glutamate in the gut. *Am J Clin Nutr* 90: 850S–856S, 2009. doi:10.3945/ajcn.2009.27462Y.
13. **Camargo SM, Singer D, Makrides V, Huggel K, Pos KM, Wagner CA, Kuba K, Danilczyk U, Skovby F, Kleta R, Penninger JM, Verrey F.** Tissue-specific amino acid transporter partners ACE2 and collectrin differentially interact with hartnup mutations. *Gastroenterology* 136: 872–882.e3, 2009. doi:10.1053/j.gastro.2008.10.055.
14. **Cassano GB, Hansson E.** Uptake of [14C]glutamine in the tissues of the mouse studied by whole-body autoradiography. *J Neurochem* 12: 851–855, 1965. doi:10.1111/j.1471-4159.1965.tb10270.x.
15. **Chan K, Busque SM, Sailer M, Stoeger C, Bröer S, Daniel H, Rubio-Aliaga I, Wagner CA.** Loss of function mutation of the Slc38a3 glutamine transporter reveals its critical role for amino acid metabolism in the liver, brain, and kidney. *Pflugers Arch* 468: 213–227, 2016. doi:10.1007/s00424-015-1742-0.

16. **Coloff JL, Murphy JP, Braun CR, Harris IS, Shelton LM, Kami K, Gygi SP, Selfors LM, Brugge JS.** Differential glutamate metabolism in proliferating and quiescent mammary epithelial cells. *Cell Metab* 23: 867–880, 2016. doi:10.1016/j.cmet.2016.03.016.
17. **Crook RB, Louie M, Deuel TF, Tomkins GM.** Regulation of glutamine synthetase by dexamethasone in hepatoma tissue culture cells. *J Biol Chem* 253: 6125–6131, 1978.
18. **Crozier SJ, D'Alecy LG, Ernst SA, Ginsburg LE, Williams JA.** Molecular mechanisms of pancreatic dysfunction induced by protein malnutrition. *Gastroenterology* 137: 1093–1101.e3, 2009. doi:10.1053/j.gastro.2009.04.058.
19. **Curthoys NP, Moe OW.** Proximal tubule function and response to acidosis. *Clin J Am Soc Nephrol* 9: 1627–1638, 2014. doi:10.2215/CJN.10391012.
20. **Dolgodilina E, Imobersteg S, Laczko E, Welt T, Verrey F, Makrides V.** Brain interstitial fluid glutamine homeostasis is controlled by blood-brain barrier SLC7A5/LAT1 amino acid transporter. *J Cereb Blood Flow Metab* 36: 1929–1941, 2016. doi:10.1177/0271678X15609331.
21. **Durán RV, Oppliger W, Robitaille AM, Heiserich L, Skendaj R, Gottlieb E, Hall MN.** Glutaminolysis activates Rag-mTORC1 signaling. *Mol Cell* 47: 349–358, 2012. doi:10.1016/j.molcel.2012.05.043.
22. **Fan MZ, Matthews JC, Etienne NM, Stoll B, Lackeyram D, Burrin DG.** Expression of apical membrane L-glutamate transporters in neonatal porcine epithelial cells along the small intestinal crypt-villus axis. *Am J Physiol Gastrointest Liver Physiol* 287: G385–G398, 2004. doi:10.1152/ajpgi.00232.2003.
23. **Fanjul C, Barrenetxe J, Lostao MP, Ducroc R.** Modulation of intestinal L-glutamate transport by luminal leptin. *J Physiol Biochem* 71: 311–317, 2015. doi:10.1007/s13105-015-0414-z.
24. **Foitzik T, Stufler M, Hotz HG, Klinnert J, Wagner J, Warshaw AL, Schulzke JD, Fromm M, Buhr HJ.** Glutamine stabilizes intestinal permeability and reduces pancreatic infection in acute experimental pancreatitis. *J Gastrointest Surg* 1: 40–46, 1997.
25. **Fukushima D, Doi H, Fukushima K, Katsura K, Ogawa N, Sekiguchi S, Fujimori K, Sato A, Satomi S, Ishida K, Fukushima K.** Glutamate exocrine dynamics augmented by plasma glutamine and the distribution of amino acid transporters of the rat pancreas. *J Physiol Pharmacol* 61: 265–271, 2010.
26. **Gammelsaeter R, Coppola T, Marcaggi P, Storm-Mathisen J, Chaudhry FA, Attwell D, Regazzi R, Gundersen V.** A role for glutamate transporters in the regulation of insulin secretion. *PLoS One* 6: e22960, 2011. doi:10.1371/journal.pone.0022960.
27. **Gao P, Tchernyshyov I, Chang TC, Lee YS, Kita K, Ochi T, Zeller KI, De Marzo AM, Van Eyk JE, Mendell JT, Dang CV.** c-Myc suppression of miR-23a/b enhances mitochondrial glutaminase expression and glutamine metabolism. *Nature* 458: 762–765, 2009. doi:10.1038/nature07823.
28. **Gheni G, Ogura M, Iwasaki M, Yokoi N, Minami K, Nakayama Y, Harada K, Hastoy B, Wu X, Takahashi H, Kimura K, Matsubara T, Hoshikawa R, Hatano N, Sugawara K, Shibasaki T, Inagaki N, Bamba T, Mizoguchi A, Fukusaki E, Rorsman P, Seino S.** Glutamate acts as a key signal linking glucose metabolism to incretin/cAMP action to amplify insulin secretion. *Cell Reports* 9: 661–673, 2014. doi:10.1016/j.celrep.2014.09.030.
29. **Graf R, Valeri F, Gassmann R, Hailemariam S, Frick TW, Bimmler D.** Adaptive response of the rat pancreas to dietary substrates: parallel regulation of trypsinogen and pancreatic secretory trypsin inhibitor. *Pancreas* 21: 181–190, 2000. doi:10.1097/00006676-200008000-00012.
30. **Guo L, Lichten LA, Ryu MS, Liuzzi JP, Wang F, Cousins RJ.** STAT5-glucocorticoid receptor interaction and MTF-1 regulate the expression of ZnT2 (Slc30a2) in pancreatic acinar cells. *Proc Natl Acad Sci USA* 107: 2818–2823, 2010. doi:10.1073/pnas.0914941107.
31. **Han T, Li X, Cai D, Zhong Y, Chen L, Geng S, Yin S.** Effect of glutamine on apoptosis of intestinal epithelial cells of severe acute pancreatitis rats receiving nutritional support in different ways. *Int J Clin Exp Pathol* 6: 503–509, 2013.
32. **Hensley CT, Wasti AT, DeBerardinis RJ.** Glutamine and cancer: cell biology, physiology, and clinical opportunities. *J Clin Invest* 123: 3678–3684, 2013. doi:10.1172/JCI69600.
33. **Høy M, Maechler P, Efanov AM, Wollheim CB, Berggren PO, Gromada J.** Increase in cellular glutamate levels stimulates exocytosis in pancreatic beta-cells. *FEBS Lett* 531: 199–203, 2002. doi:10.1016/S0014-5793(02)03500-7.
34. **Hu W, Zhang C, Wu R, Sun Y, Levine A, Feng Z.** Glutaminase 2, a novel p53 target gene regulating energy metabolism and antioxidant function. *Proc Natl Acad Sci USA* 107: 7455–7460, 2010. doi:10.1073/pnas.1001006107.
35. **Iñigo C, Barber A, Lostao MP.** Na^+ and pH dependence of proline and beta-alanine absorption in rat small intestine. *Acta Physiol (Oxf)* 186: 271–278, 2006. doi:10.1111/j.1748-1716.2006.01538.x.
36. **Iwanaga T, Goto M, Watanabe M.** Cellular distribution of glutamate transporters in the gastrointestinal tract of mice: an immunohistochemical and in situ hybridization approach. *Biomed Res* 26: 271–278, 2005. doi:10.2220/biomedres.26.271.
37. **Janeczko MJ, Stoll B, Chang X, Guan X, Burrin DG.** Extensive gut metabolism limits the intestinal absorption of excessive supplemental dietary glutamate loads in infant pigs. *J Nutr* 137: 2384–2390, 2007. doi:10.1093/jn/137.11.2384.
38. **Kirchhoff P, Dave MH, Remy C, Kosiek O, Busque SM, Dufner M, Geibel JP, Verrey F, Wagner CA.** An amino acid transporter involved in gastric acid secretion. *Pflugers Arch* 451: 738–748, 2006. doi:10.1007/s00424-005-1507-2.
39. **Lawrence CB, Davies NT.** A novel, simple and rapid method for the isolation of mitochondria which exhibit respiratory control, from rat small intestinal mucosa. *Biochim Biophys Acta* 848: 35–40, 1986. doi:10.1016/0005-2728(86)90157-X.
40. **Loayza-Puch F, Drost J, Rooijers K, Lopes R, Elkon R, Agami R.** p53 induces transcriptional and translational programs to suppress cell proliferation and growth. *Genome Biol* 14: R32, 2013. doi:10.1186/gb-2013-14-4-r32.
41. **Love AH.** Metabolic response to malnutrition: its relevance to enteral feeding. *Gut* 27, *Suppl* 1: 9–13, 1986. doi:10.1136/gut.27.Suppl_1.9.
42. **Lyck R, Ruderisch N, Moll AG, Steiner O, Cohen CD, Engelhardt B, Makrides V, Verrey F.** Culture-induced changes in blood-brain barrier transcriptome: implications for amino-acid transporters in vivo. *J Cereb Blood Flow Metab* 29: 1491–1502, 2009. doi:10.1038/jcbfm.2009.72.
43. **Maechler P, Wollheim CB.** Mitochondrial glutamate acts as a messenger in glucose-induced insulin exocytosis. *Nature* 402: 685–689, 1999. doi:10.1038/45280.
44. **Marquard J, Otter S, Welters A, Stirban A, Fischer A, Eglinger J, Herebian D, Kletke O, Klemen MS, Stožer A, Wnendt S, Piemonti L, Köhler M, Ferrer J, Thorens B, Schliess F, Rupnik MS, Heise T, Berggren PO, Klöcker N, Meissner T, Mayatepek E, Eberhard D, Kragl M, Lammert E.** Characterization of pancreatic NMDA receptors as possible drug targets for diabetes treatment. *Nat Med* 21: 363–372, 2015. doi:10.1038/nm.3822.
45. **Morales A, Buenabad L, Castillo G, Vazquez L, Espinoza S, Htoo JK, Cervantes M.** Dietary levels of protein and free amino acids affect pancreatic proteases activities, amino acids transporters expression and serum amino acid concentrations in starter pigs. *J Anim Physiol Anim Nutr (Berl)*, 101: 723–732, 2017. doi:10.1111/jpn.12515.
46. **Nakamura H, Kawamata Y, Kuwahara T, Torii K, Sakai R.** Nitrogen in dietary glutamate is utilized exclusively for the synthesis of amino acids in the rat intestine. *Am J Physiol Endocrinol Metab* 304: E100–E108, 2013. doi:10.1152/ajpendo.00331.2012.
47. **Nardi F, Hoffmann TM, Stretton C, Cwiklinski E, Taylor PM, Hundal HS.** Proteasomal modulation of cellular SNAT2 (SLC38A2) abundance and function by unsaturated fatty acid availability. *J Biol Chem* 290: 8173–8184, 2015. doi:10.1074/jbc.M114.625137.
48. **Norman K, Pichard C, Lochs H, Pirlich M.** Prognostic impact of disease-related malnutrition. *Clin Nutr* 27: 5–15, 2008. doi:10.1016/j.clnu.2007.10.007.
49. **Otter S, Lammert E.** Exciting times for pancreatic islets: glutamate signaling in endocrine cells. *Trends Endocrinol Metab* 27: 177–188, 2016. doi:10.1016/j.tem.2015.12.004.
50. **Qing G, Li B, Vu A, Skuli N, Walton ZE, Liu X, Mayes PA, Wise DR, Thompson CB, Maris JM, Hogarty MD, Simon MC.** ATF4 regulates MYC-mediated neuroblastoma cell death upon glutamine deprivation. *Cancer Cell* 22: 631–644, 2012. doi:10.1016/j.ccr.2012.09.021.
51. **Qu W, Oya S, Lieberman BP, Ploessl K, Wang L, Wise DR, Divgi CR, Chodosh LA, Thompson CB, Kung HF.** Preparation and characterization of L-[5-11C]-glutamine for metabolic imaging of tumors. *J Nucl Med* 53: 98–105, 2012. [Erratum. *J Nucl Med* 53: 646, 2012.] doi:10.2967/jnumed.111.093831.
52. **Reeds PJ, Burrin DG, Stoll B, Jahoor F.** Intestinal glutamate metabolism. *J Nutr* 130, *Suppl*: 978S–982S, 2000. doi:10.1093/jn/130.4.978S.

53. **Reid MA, Wang WI, Rosales KR, Welliver MX, Pan M, Kong M.** The B55α subunit of PP2A drives a p53-dependent metabolic adaptation to glutamine deprivation. *Mol Cell* 50: 200–211, 2013. doi:10.1016/j.molcel.2013.02.008.
54. **Ritchie JW, Baird FE, Christie GR, Stewart A, Low SY, Hundal HS, Taylor PM.** Mechanisms of glutamine transport in rat adipocytes and acute regulation by cell swelling. *Cell Physiol Biochem* 11: 259–270, 2001. doi:10.1159/000047812.
55. **Rooman I, Lutz C, Pinho AV, Huggel K, Reding T, Lahoutte T, Verrey F, Graf R, Camargo SM.** Amino acid transporters expression in acinar cells is changed during acute pancreatitis. *Pancreatology* 13: 475–485, 2013. doi:10.1016/j.pan.2013.06.006.
56. **Rose PM, Hopper AF, Wannemacher RW Jr.** Cell population changes in the intestinal mucosa of protein-depleted or starved rats. I. Changes in mitotic cycle time. *J Cell Biol* 50: 887–892, 1971. doi:10.1083/jcb.50.3.887.
57. **Schachter D, Buteau J.** Glutamate formation via the leucine-to-glutamate pathway of rat pancreas. *Am J Physiol Gastrointest Liver Physiol* 306: G938–G946, 2014. doi:10.1152/ajpgi.00394.2013.
58. **Smilowitz JT, O'Sullivan A, Barile D, German JB, Lönnerdal B, Slupsky CM.** The human milk metabolome reveals diverse oligosaccharide profiles. *J Nutr* 143: 1709–1718, 2013. doi:10.3945/jn.113.178772.
59. **Son J, Lyssiotis CA, Ying H, Wang X, Hua S, Ligorio M, Perera RM, Ferrone CR, Mullarky E, Shyh-Chang N, Kang Y, Fleming JB, Bardeesy N, Asara JM, Haigis MC, DePinho RA, Cantley LC, Kimmelman AC.** Glutamine supports pancreatic cancer growth through a KRAS-regulated metabolic pathway. *Nature* 496: 101–105, 2013. [Erratum. *Nature* 499: 504, 2013.] doi:10.1038/nature12040.
60. **Sonda S, Silva AB, Grabliauskaite K, Saponara E, Weber A, Jang JH, Züllig RA, Bain M, Reding Graf T, Hehl AB, Graf R.** Serotonin regulates amylase secretion and acinar cell damage during murine pancreatitis. *Gut* 62: 890–898, 2013. doi:10.1136/gutjnl-2011-301724.
61. **Stoll B, Burrin DG, Henry J, Yu H, Jahoor F, Reeds PJ.** Substrate oxidation by the portal drained viscera of fed piglets. *Am J Physiol Endocrinol Metab* 277: E168–E175, 1999. doi:10.1152/ajpendo.1999.277.1E168.
62. **Tapiero H, Mathé G, Couvreur P, Tew KD.** II. Glutamine and glutamate. *Biomed Pharmacother* 56: 446–457, 2002. doi:10.1016/S0753-3322(02)00285-8.
63. **Van der Schoor SR, van Goudoever JB, Stoll B, Henry JF, Rosenberger JR, Burrin DG, Reeds PJ.** The pattern of intestinal substrate oxidation is altered by protein restriction in pigs. *Gastroenterology* 121: 1167–1175, 2001. doi:10.1053/gast.2001.29334.
64. **Walls AB, Waagepetersen HS, Bak LK, Schousboe A, Sonnewald U.** The glutamine-glutamate/GABA cycle: function, regional differences in glutamate and GABA production and effects of interference with GABA metabolism. *Neurochem Res* 40: 402–409, 2015. doi:10.1007/s11064-014-1473-1.
65. **Windmueller HG, Spaeth AE.** Intestinal metabolism of glutamine and glutamate from the lumen as compared to glutamine from blood. *Arch Biochem Biophys* 171: 662–672, 1975. doi:10.1016/0003-9861(75)90078-8.
66. **Windmueller HG, Spaeth AE.** Respiratory fuels and nitrogen metabolism in vivo in small intestine of fed rats. Quantitative importance of glutamine, glutamate, and aspartate. *J Biol Chem* 255: 107–112, 1980.
67. **Wise DR, DeBerardinis RJ, Mancuso A, Sayed N, Zhang XY, Pfeiffer HK, Nissim I, Daikhin E, Yudkoff M, McMahon SB, Thompson CB.** Myc regulates a transcriptional program that stimulates mitochondrial glutaminolysis and leads to glutamine addiction. *Proc Natl Acad Sci USA* 105: 18782–18787, 2008. doi:10.1073/pnas.0810199105.
68. **Xiang L, Xie G, Liu C, Zhou J, Chen J, Yu S, Li J, Pang X, Shi H, Liang H.** Knock-down of glutaminase 2 expression decreases glutathione, NADH, and sensitizes cervical cancer to ionizing radiation. *Biochim Biophys Acta* 1833: 2996–3005, 2013. doi:10.1016/j.bbamcr.2013.08.003.
69. **Xiao D, Ren P, Su H, Yue M, Xiu R, Hu Y, Liu H, Qing G.** Myc promotes glutaminolysis in human neuroblastoma through direct activation of glutaminase 2. *Oncotarget* 6: 40655–40666, 2015. doi:10.18632/oncotarget.5821.
70. **Xiao W, Feng Y, Holst JJ, Hartmann B, Yang H, Teitelbaum DH.** Glutamate prevents intestinal atrophy via luminal nutrient sensing in a mouse model of total parenteral nutrition. *FASEB J* 28: 2073–2087, 2014. doi:10.1096/fj.13-238311.
71. **Yang C, Ko B, Hensley CT, Jiang L, Wasti AT, Kim J, Sudderth J, Calvaruso MA, Lumata L, Mitsche M, Rutter J, Merritt ME, DeBerardinis RJ.** Glutamine oxidation maintains the TCA cycle and cell survival during impaired mitochondrial pyruvate transport. *Mol Cell* 56: 414–424, 2014. doi:10.1016/j.molcel.2014.09.025.
72. **Yang H, Wang X, Xiong X, Yin Y.** Energy metabolism in intestinal epithelial cells during maturation along the crypt-villus axis. *Sci Rep* 6: 31917, 2016. doi:10.1038/srep31917.
73. **Yilmaz OH, Katajisto P, Lamming DW, Gültekin Y, Bauer-Rowe KE, Sengupta S, Birsoy K, Dursun A, Yilmaz VO, Selig M, Nielsen GP, Mino-Kenudson M, Zukerberg LR, Bhan AK, Deshpande V, Sabatini DM.** mTORC1 in the Paneth cell niche couples intestinal stem-cell function to calorie intake. *Nature* 486: 490–495, 2012. doi:10.1038/nature11163.
74. **Zhou Y, Waanders LF, Holmseth S, Guo C, Berger UV, Li Y, Lehre AC, Lehre KP, Danbolt NC.** Proteome analysis and conditional deletion of the EAAT2 glutamate transporter provide evidence against a role of EAAT2 in pancreatic insulin secretion in mice. *J Biol Chem* 289: 1329–1344, 2014. doi:10.1074/jbc.M113.529065.
75. **Zielińska M, Dąbrowska K, Hadera MG, Sonnewald U, Albrecht J.** System N transporters are critical for glutamine release and modulate metabolic fluxes of glucose and acetate in cultured cortical astrocytes: changes induced by ammonia. *J Neurochem* 136: 329–338, 2016. doi:10.1111/jnc.13376.